LUPINE PUBLISHERS

Journal Of Anthropological And Archaeological Sciences

DOI: 10.32474/JAAS.2023.08.000286

ISSN: 2690-5752

Research Article

Multidisciplinary Geological-Geophysical Analysis Unmasks Anthropological Site Structure in the Northern Part of the Levantine Corridor

Lev Eppelbaum[1,2]* and Youri Katz[3]

[1]*School of Geosciences, Faculty of Exact Sciences, Tel Aviv University, Israel*

[2]*Azerbaijan State Oil and Industry University, Azadlig Ave. 20, Baku AZ1010, Azerbaijan, Israel*

[3]*Steinhardt Museum of Natural History & National Research Center, Faculty of Life Sciences, Tel Aviv University, Israel*

***Corresponding author:** Lev Eppelbaum, School of Geosciences, Faculty of Exact Sciences, Tel Aviv University, Ramat Aviv 6997801, Tel Aviv, Azerbaijan State Oil and Industry University, Israel

Received: June 02, 2023 **Published:** June 13, 2023

Abstract

The study of the ancient anthropological sites of the Levantine Corridor is very significant for understanding the evolution of ancient hominins and the time of their dispersal from East Africa to the Caucasus and Eurasia. The event stratigraphy data and paleomagnetic studies of the latest Cenozoic are comprehensively generalized for the Levantine region. Compiled integrated structural-paleomagnetic-event stratigraphic chart enabled the exact correlation of the northern Levantine ancient hominin sites. For a thorough analysis of the well-studied anthropological site of 'Ubeidiya (located some km SW of the Sea of Galilee), we used the following principal methodologies: paleogeographic research combined with examination of hydrospheric disturbances, analysis of cyclic stratigraphy, generalization of detailed paleomagnetic stratigraphy, biostratigraphic correlation, lithological-facies analysis, event stratigraphy, and structural-tectonic studies. Methods of comparative analysis of several anthropological sites surrounding the site of 'Ubeidiya were also employed. Comprehensive paleomagnetic mapping and profiling have been applied to a few areas in the northern part of the Levantine corridor. It can reveal some essential tectonic-structural peculiarities of the sites disposed of this strip. Paleogeographic and tectonic-geodynamic data analyses indicate that the Calabrian age of the 'Ubeidiya site is discussable. The constructed palinspastic reconstruction map (3.6 - 2.0 Ma) unmasked important tectonic-magmatic features of the area under study. Based on the combined multifactor analysis, we propose that the age of this site can be significantly increased. The new suggested age (Lower Matuyama - Gelasian) may require a revision of the entire global process of dispersal of primitive man from Africa to the north.

Keywords: Paleogeographic examination; event stratigraphy; paleomagnetic correlation; paleomagnetic mapping; landscape studies; chronostratigraphic studies; palinspastic reconstruction; combined interpretation

Introduction

The sites of the ancient hominins of the Levantine region are very significant for assessing the evolution of early hominins and the time of their dispersal from East Africa [1-3]. The relationship between archaeological and geological-geophysical studies is associated with determining the age of sites and the paleogeographic conditions in which they were formed. Most of the studies of sedimentation complexes containing early hominin sites are based on a relatively narrow range of physical-chemical, paleontological, and archaeological methods. The age of the most ancient sites in the Levant ranges from 2.0 to 1.1 Ma, while in East Africa, it is 2.6-2.4 Ma, and in the Caucasus region, it is 2.1-1.7 Ma [4]. Such a scatter in the age range of sites with the most ancient artifacts indicates that the methods' scope does not give unambiguous correlation results. It requires an assessment from the standpoint of both general and re-

gional stratigraphy under the conditions of different facies characteristics of the sections. The location of some of the ancient anthropological sites in the Levant is shown in Figure 1. One of the most important sites is the well-studied multi-layered site of 'Ubeidiya [e.g., 5,6], located a few km SW of the Sea of Galilee (Kinnarot Basin). The age of this site was determined as 1.6-1.4 Ma [6].

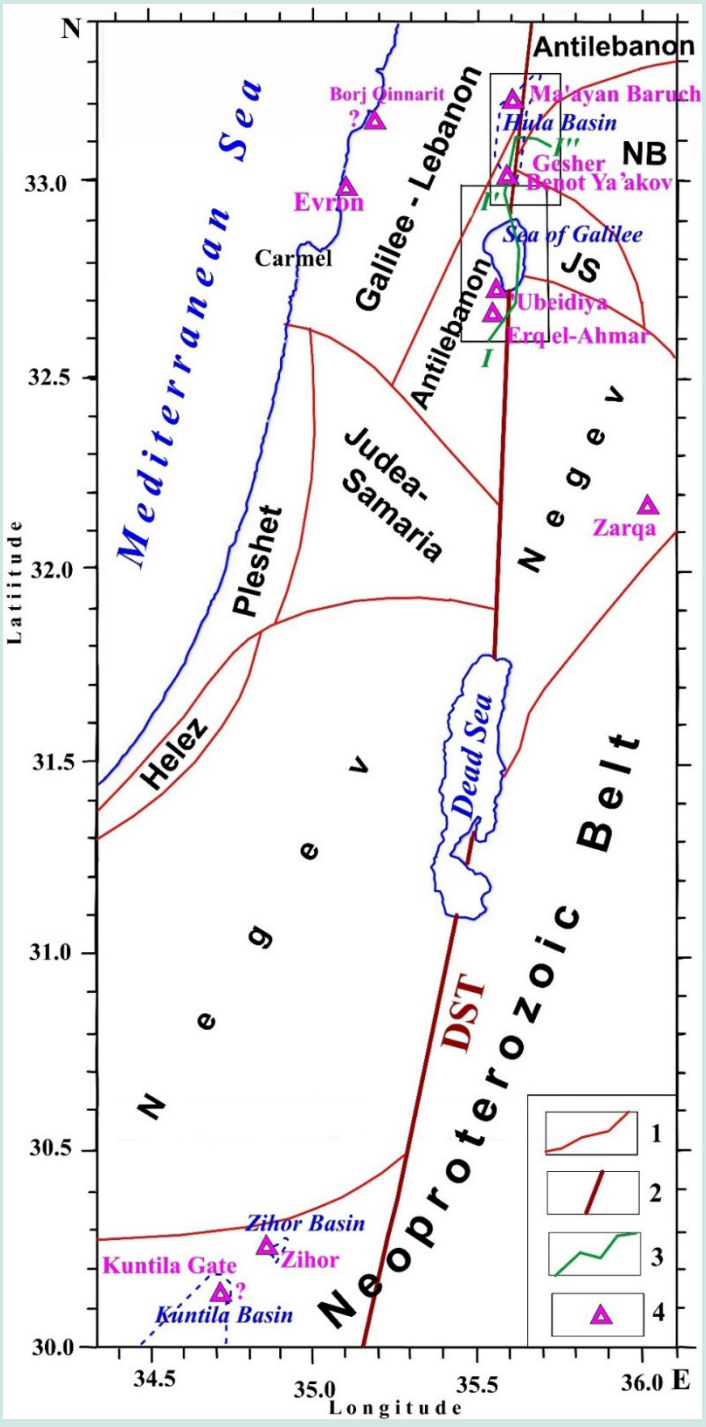

Figure 1: A simplified tectonic map of the studied region with the location of studied ancient hominin sites. (1) intraplate faults, (2) interplate faults, (3) location of the paleomagnetic profile, (4) ancient archaeological sites. DST, Dead Sea Transform, JS, Judea-Samaria, NB, Neoproterozoic Belt. The dotted lines contour the Kuntila and Hula basins. The symbols I, I' and I'' designate the position of the paleomagnetic profile in Figures 6 and 7 and the various parts of the paleomagnetic profile in Figure 8. Symbol '?' indicates insufficient knowledge of the geological section.

The ages of the anthropological sites and attracted geological sections are estimated by stratigraphic, radiometric, paleomagnetic, anthropological, and paleogeographic methods. Among the latter, the most important are the nature of the land-sea ratio (analysis of transgressions and regressions) and the stages of climate change (see subsections 3.1 - 3.3). To solve the first problem, we used the method of hydrospheric disturbances [7] based on measurements of the levels of sea terraces and the amplitude of river incisions (Figure 2). This method shows the best results in the relatively stable areas of continental platforms. Tectonic-paleomagnetic mapping in the area of widespread development of the Late Cenozoic deposits containing numerous sites of ancient hominins requires a thorough analysis of tectonic, geodynamic, paleomagnetic, and other geological events (see subsections 3.4 - 3.5). On their basis, the mapping itself and the study of the abiotic habitat of ancient hominin are carried out, and the sites' ages are estimated. For this purpose, we analyzed the identified general chronostratigraphic scale. Then we correlated the heterogeneous elements of the Late Cenozoic event and paleomagnetic stratigraphy for the Levant and Paratethys basins.

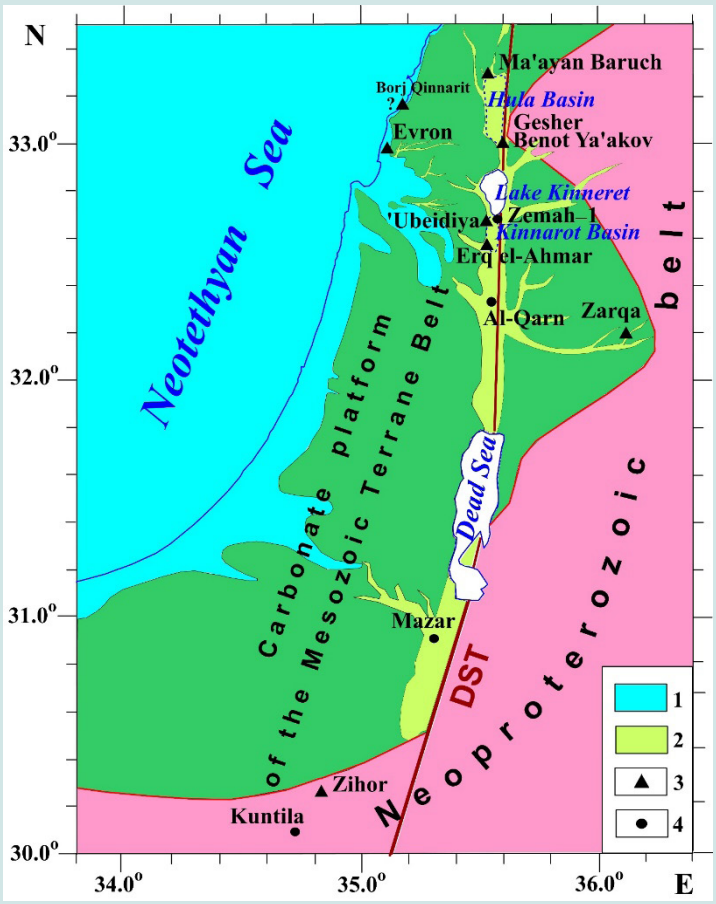

Figure 2: A simplified tectonic-paleogeographic map of the Levantine region for the Gelasian-Akchagylian time of the maximal flooding. (1) areas covered by the Gelasian Sea of Neotethys, (2) areas of the development of alluvial and lacustrine facies of the Gelasian stage, (3) location of the archaeological sites of the ancient hominins considered in the presented study, (4) location of geological sections Kuntila and Mazar (southern Israel), and Zemah-1 borehole (northern Israel) significant for the radiometric, stratigraphic, and paleomagnetic correlation. DST, Dead Sea Transform. Symbol '?' indicates insufficient knowledge of geological-archaeological data.

Materials and Methods

Materials

In this research were used the previous authors' investigations [7-19], results of the authors' field surveys in the area, and numerous studies of other authors in the fields of magnetostratigraphy [20-31], paleomagnetic analyses [32-42], radiometric dating [34,39,41,43-52], tectonics [32,34,45,47-49,52-64], stratigraphy [41,55,60,65], paleontology [66-70], geological-geophysical mapping [59,60,64,71-74], and archaeological and anthropological data [1-3,5,6,37,41,66,69,70, 75-82].

Methods

The study of such complex ancient anthropological sites requires their analysis using the integration of reliable, comprehensive methods. The variety of geophysical, geological, and paleon-

tological methods (including compilation results) employed in this investigation are presented in Figure 3. For the first time, in the region under study was used a combined analysis of physical (radiometric, magnetostratigraphic, paleomagnetic correlation, paleomagnetic mapping, and geodynamical analysis), geological (lithofacies, event stratigraphy, hydrospheric disturbances, cyclic stratigraphy, paleogeographical, magmatic activations, and palinspastic reconstructions), and paleontological (biostratigraphic correlation and ecostratigraphic analysis) methods.

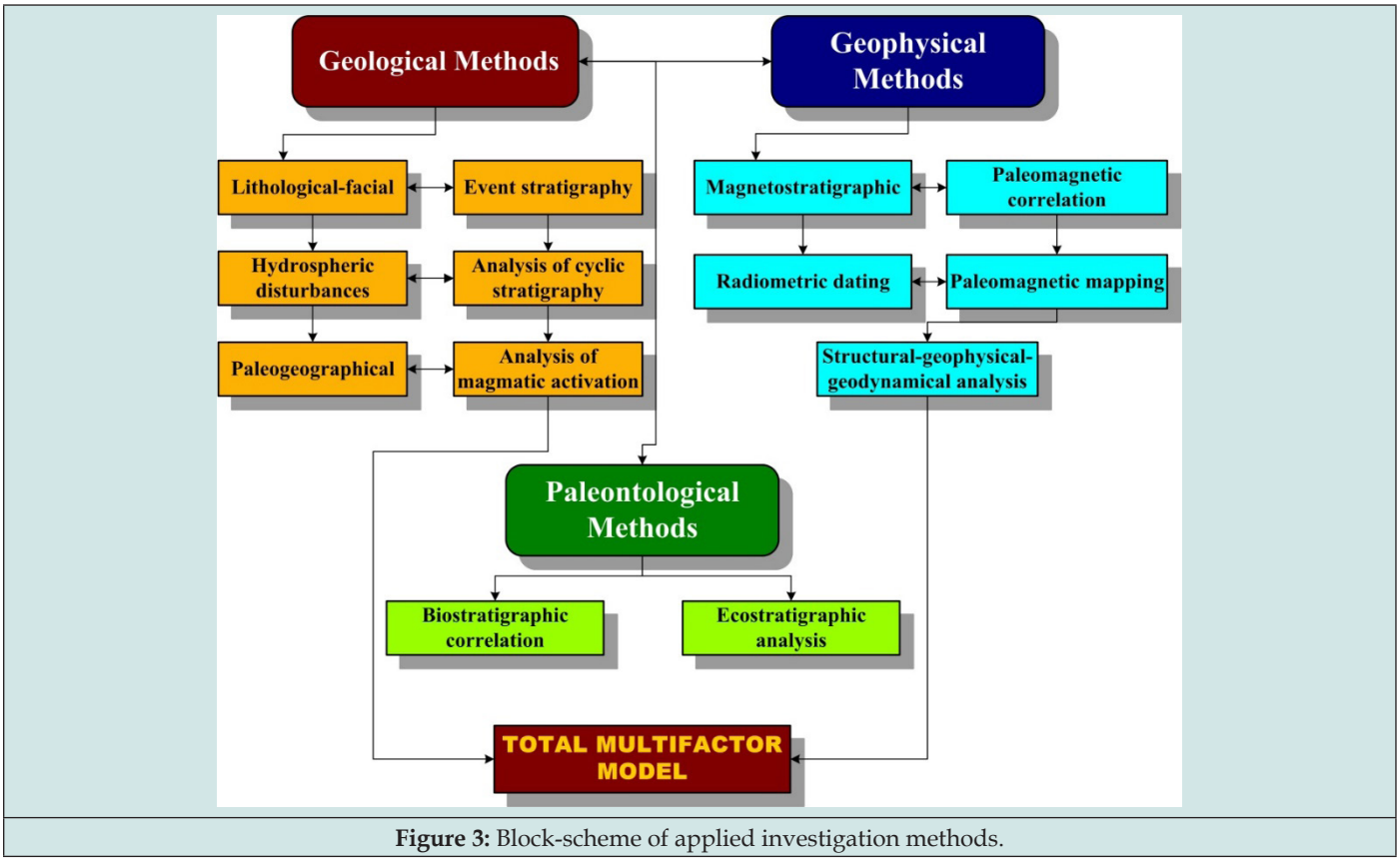

Figure 3: Block-scheme of applied investigation methods.

Principal preferences of integrated interpretation

It is well known that an integrated examination (sensing) increases the amount and reliability of geophysical-geological information sharply [83,84]. Theoretically, suppose a set of geophysical (geological, geochemical, archaeological) methods is focused on investigating independent indicators of equal value. In that case, the anomaly detection reliability γ can be described by an equation.

$$\gamma = F\left(\frac{\sqrt{\sum_i \upsilon_i}}{2}\right)$$

where υ is the ratio of the anomaly squared to the noise dispersion for each i-th method, and F is the probability integral.

Let us assume that three points indicate some natural anomaly and that the mean square of the anomaly for each field is equal to the noise dispersion. For a single investigation method, the reliability of detecting an anomaly of a known form and intensity can be calculated by Kotelnikov's criterion [e.g., 85]. Hence the reliability for individual methods is 0.61 and 0.77, and 0.87 for a set of two or three methods, respectively. It means that the q value (risk of an erroneous solution, $q = 1 - \gamma$) decreases when integrating two or three methods by factors of 1.7 and 3.0, respectively. These simple calculations indicate the preferences of different method integration. In our subsurface sensing, the number of applied methods with positive estimations in many cases vastly outnumbers the three. The presented multidisciplinary study covers more than ten independent geological and geophysical methods, making the obtained results sufficiently reliable.

Results

Analysis of the event-stratigraphic, paleomagnetic and tectonic-thermal events

The Levant region is a tectonic structure occurring between the African-Arabian and South European regions. The complexity of this structure is associated with the developed here initial stages of rifting and the final phases of the collision of the Neotethys Ocean [4]. Tectonic-thermal events were most clearly manifested in the area of the largest Late Cenozoic trap field in the Middle East, the Ash Shaam field, and the Dead Sea Transform (DST) area is

the reference and most studied petrologically and radiometrically. A detailed analysis of paleomagnetic stratigraphy can provide interpretative possibilities that no other geological and geophysical methods deliver [12]. The determination of the sequence of Chrons, subchrons, and more fractional magnetostratigraphic divisions of the Upper Cenozoic of the study region was compiled from the Middle Miocene to the Holocene (Figure 4a). The second column (Figure 4b) shows the geochronological scale, Chrons, and subchrons of the magnetostratigraphic scale, for which the proper names and alphanumeric indices are used.

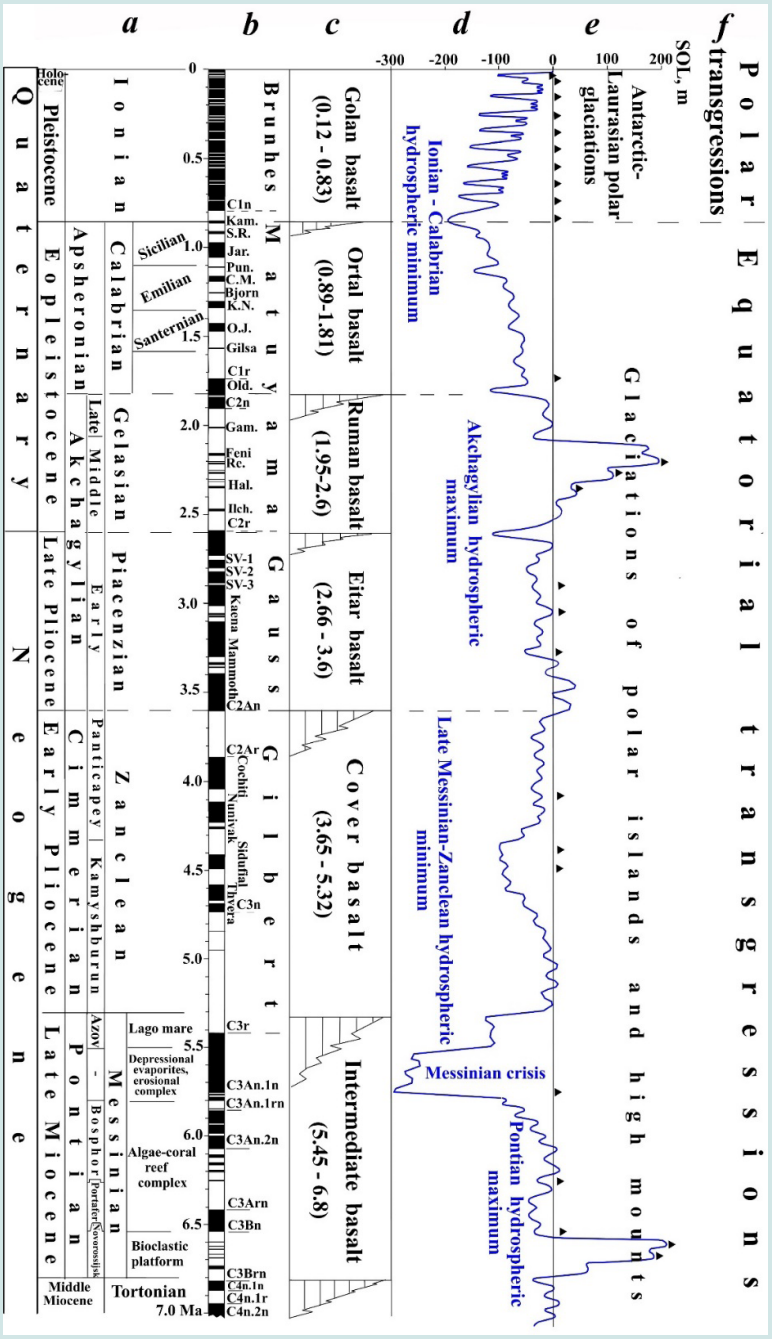

Figure 4: Paleomagnetic and event stratigraphy of the latest Cenozoic of the Levantine region compared with the Tethyan-Paratethyan scale and paleogeographic-geodynamic events: a – stratigraphic scale, b – magnetostratigraphic scale, c – the scale of magmatic events of the Harrat Ash Shaam, d – hydrospheric events, e – cryospheric events, f – events of the Earth's figure changes. SOL, Standard Ocean Level.

Paleomagnetic subchrons: Kam., Kamikatsura, S.R., Santa Roza, Jar., Jaramillo, Pun., Punaruu, C.M., Cobb Mt., K.N., Kvemo-Natanebi, O.J., Ontong Java, Old., Olduvai, Gam., Gamarri, Feni, Re., Reunion, Hal., Halawa, Ilch., Ilchembet (?), SV (1-3), Searles Valley (1-3). The paleomagnetic data were generalized based on [6,22,25,27,28,35,36,40–42,66]. The ages of basalts were generalized based on [34,48,52,57,60].

The Gilbert, Gauss, Matuyama, and Brunhes Chrons are distinguished here [e.g., 19,24,25,27]. They form natural cycles which are comparable to the tiers of the Mediterranean scale. For instance, Gilbert Chron corresponds to Zanclean, Gauss Chron to Piacenzian, Matuyama Chron to Gelasian and Calabrian, and Brunhes Chron to Ionian (Figures 4a & 4b). Careful magnetostratigraphic and tectonic-paleogeographic analysis of the 'Ubeidiya anthropological site indicates that its age may relate to the Calabrian or Gelasian. However, reliable assessment of the paleomagnetic age of archaeological sites is currently problematic. This circumstance is due to many factors. The magnetostratigraphic scale indexation is based on the finely determined structure of the geomagnetic field [20,23-25,29,30] and its astronomical and oxygen isotope calibration [27,28,31]. The involvement of these data serves as the basis for the relation of paleomagnetically dated archaeological sites to one or another segment of the modernized magnetostratigraphic scale (Figure 4b).

Performed review of the literature indicated that the lower part of the paleomagnetic Matuyama Chron has not been studied enough [e.g., 27,30]. Therefore, for the correct compilation of the magnetostratigraphic scale (Figure 4b), such classical geological methods as biostratigraphic correlation, lithological, facies, and structural-tectonic analysis, and event stratigraphy were applied [21,22,26,28,30]. The dominance of reverse polarity distinguishes Gilbert Chron. It precedes the Gauss Chron, where normal polarity prevails, and then the Matuyama Chron, where relatively short subchrons of normal polarity dominate against the background of reverse polarity, except for the Olduvai subchron in the middle part of this zone (Figure 4b). The Brunhes Chron of normal polarity contains numerous short-term subchrons of the normal and alternating polarity and is not completed.

Numerous subdivisions of trap complexes were identified and classified in the Golan Plateau, the Southern Galilee, and the Hula, Kinneret, and Jordan basins [14,19]. After this, they grouped into larger magnetostratigraphic divisions that received the above names (Figure 4c). These sequences of basalt traps form the natural tectonic-thermal stages separated by breaks. Tectonic-thermal events, their corresponding stratigraphic units, and rock complexes in this region are associated with its active plate geodynamics (Figure 4c). They manifested themselves most clearly at the boundary of the Arabian and Sinai plates within the largest trap field in the Middle East, Harrat Ash Shaam [52,60]. In general, a regular cyclicity of the intensity and type of tectonic-thermal events is revealed in the region [13]. It consists, for instance, of the areal development of trap complexes and the replacement of intrusive magmatism with effusive one [4].

In the late Cenozoic, the most stable, extensive trap volcanism and regional uplifts appeared in the Early Pliocene (Zanclean), when the Cover Basalts of the Lower Galilee, the southern part of the Golan Plateau, and a significant part of the DST zone from the Korazim Plateau to the Kinneret and Kinnarot troughs were formed [57]. The second considerable peak of tectonic-thermal events is associated with active volcanism of the Calabrian and Ionian stages, manifested in the northern part of the Golan Plateau near the boundary of the Precambrian massif of the Arabian Plate and the Mesozoic Terrane Belt [13]. Tectonic-thermal events, which actively influenced the landscape formation, climate, the evolution of ecosystems, and the settlement of ancient people, clearly correlate with the regional geological-geophysical processes [e.g., 7]. Based on these positions, the critical factors controlling the settlement of ancient man are the weakening of volcanism and the development of tectonic depressions with optimal landscapes for the habitation of ancient man. In this respect, the stage of tectonic-thermal events between the Cover Basalts and Ortal-Golan Basalts (Figure 4c) corresponds to a minimum of volcanic activity and a maximum of subsidence with the formation of depression alluvial-depression strata. This one corresponds to the Akchagylian stage (Figure 4d).

In this paper, for the first time, we point out that these cycles of the Levant trap series coincide completely with the latest Cenozoic stages identified in marine sections of the Mediterranean. Intermediate Basalts correspond to the Messinian Stage, Cover Basalts to Zanclean, Eitar Basalts to Piacenzian, Ruman Basalts to Gelasian, Ortal Basalts to Calabrian, and Golan Basalts to Ionian (Figure 4c). The presented correlation has significant importance since the wide volcanism's development in the Levantine corridor has influenced the dispersal of the early hominins from Eastern Africa. These data will be used later for constructing paleomagnetic columns and maps.

A brief analysis of hydrospheric disturbances

The hydrospheric disturbances in this region were studied earlier [7,13]. The Late Miocene-Messinian stage formed a wave of hydrosphere fluctuations from +200 to -300 m (Figure 4d) relative to the current world sea level [7,86,87]. The initial extremum in the range of 6.75-6.5 Ma corresponds to the Pontic transgressive peak known in the Euxine Paratethys basin and developed in the Levantine region in the form of carbonates of the Bira Formation and deposition of saline strata in the DST basins. During most of the Messinian epoch, the sea basin level corresponded to the current level, up to 5.8-5.75 Ma. After the Messinian crisis came, it was marked by a sharp drop in the level of the hydrosphere, the closure of the Tethys-Paratethys basins, and the drying of the Mediterranean Sea (Figure 4). This crisis is a unique phenomenon in the Earth's history since the land relief's descent to values of 2,000-4,000 m below the ocean level is unprecedented in paleogeographic terms. It undoubtedly influenced many geodynamically significant subsequent events in the history of the Earth, including the development of the landscape, climate, ecosystems, and the evolution of the biosphere [8].

In general, after the Messinian crisis, the level of the hydrosphere was lower than today. During Zanclean and the end of Messinian, the Tethys Basin was relatively narrow, and the spaces of the surrounding land formed an extensive arid belt. Significant paleogeographic changes manifested themselves during the epoch of the Akchagylian hydrospheric maximum [7], initially identified in the Caspian-Turanian Basin of Paratethys. In the Levant, the ex-

tremum of this transgression (up to 100-200 m above the current ocean level) covered the western part of the carbonate platform. This circumstance narrowed the optimal path of hominin dispersal from the coasts of the rift lakes of East Africa to the north to the coastal areas of the vast Tethys and Paratethys water areas [4]. The end of this great flood, followed by the hydrospheric minimum of the Calabrian-Ionian age, contributed to the development of the Levantine corridor.

Before the Ionian stage, glacial processes had no a pronounced planetary character (Figure 4e). A stable ice sheet covered only the continent of Antarctica. The transfer of excess moisture caused mountain glaciations and insular glaciers from the tropical areas to the Polar Regions under rising levels of the hydrosphere. The dominance of the glacial climate with the intensification of contrasting movements under an increase in the Earth's orbit eccentricity and the development of continental glaciations over vast expanses of Laurasia, Antarctica, and southern America began around 0.85 Ma ago [7]. Thus, glacial and planetary-geodynamic factors (Figures 4e and 4f, correspondingly) were decisive in ancient hominin settling, evolution, and sapientization.

Stratigraphic and paleogeographic evidence

We have diversified the traditional correlation criteria and methods following the current level of stratigraphic studies by introducing elements of the event and cyclic stratigraphy and criteria for paleogeographic and tectonic-geodynamic assessment of sequences containing sites of ancient hominins. These procedures were performed considering the conditions for forming previous and subsequent deposits and stratigraphic breaks. The chronostratigraphic nomenclature was regionally justified for the Mediterranean and the Paratethys basins, and local magnetostratigraphic divisions were used for the stage determination. The latter is very important for paleomagnetic stratigraphy. It is based on the most studied paleopedological scale and the benchmarks of sea-level fluctuations measured in relatively stable zones of continental platforms.

The unification of the tiered scale is crucial, considering planetary hydrospheric disturbances used for its establishment. These perturbations in the practice of archeology were considered only on the coasts. Meanwhile, they play a leading role in the landscape and climate changes since fluctuations in the final water body of flow levels are the leading cause of the evolution of vast ecosystems in which ancient hominins lived. Therefore, it is desirable to introduce the criteria of ecostratigraphy and climatostratigraphic correlation into archaeological stratigraphy, considering the alternation of humidification and drying periods (respectively, pluvial and arid epochs). In this regard, studies on the hydrogeological cycles regulating the development of ancient hominins are critical [e.g., 65]. This requires a separate detailed investigation.

The character of the Upper Cenozoic sections and the sites' distribution vary in different regions of the Eastern Mediterranean. Therefore, their tectonic-paleogeographic typification was carried out with the allocation of the coastal plain, the DST zone of troughs and uplifts, and the uplifted plateau of the Neoproterozoic Sinai massif. The first two regions are significantly differentiated in seismotectonic, landscape-structural, and facies-paleogeographic features, associated with their younger character than the igneous and metamorphic Precambrian Sinai belt. Ancient anthropological sites (we consider the primary site of 'Ubeidiya and some essential surrounding sites of Gesher Benot Yakov, Evron, Erq El-Ahmar, Zarqa, and Zihor) (Figure 2) dominate precisely in the above two areas. These areas contain various facies types of sedimentary complexes and terrestrial volcanic rocks (Figure 5).

The multi-layered structure of the site of 'Ubeidiya indicates that it was exploited for a long time, considered a stable source of fresh water, rich hunting opportunities, and plentiful potentially comestible plants [5,78]. The event-stratigraphic and rhythm-stratigraphic analyses show that the 'Ubeidiya and Erq El-Ahmar formations do not contain a significant break and form a single sequence of the lacustrine-alluvial cycles within the Gauss and Matuyama Chrons [35,36]. Within the DST trough, sections are known where analogs of the 'Ubeidiya and Erq El-Ahmar formations are developed in an Al-Qarn section in Jordan Valley [68] (Figure 2). The gastropod remains studied in this section [68] show that the gastropod assemblages in the 'Ubeidiya and Erq El-Ahmar formations are continuous into each other (Figure 5). The gastropod remains related to the same paleogeographic-sedimentological cycle, and significant breaks in the previous geological sections are unlikely to have developed.

The carbonate platform of the Eastern Mediterranean coastal plain (Figure 2) is tectonically subsided and partly forms the modern shelf of the Levant [12], contains marine sediments and, to a lesser extent, Neogene traps. On the contrary, the DST basins contain diverse traps of different ages, fresh and brackish-water lacustrine carbonate-terrigenous strata, and alluvial-soil series of river terraces. The facial complexes are presented in Figure 5 (corresponding signs to the right of the columns). The columns indicate the paleomagnetic polarity of deposits or igneous formations if they are present in the sections. At the same time, the section's completeness is indicated, considering the size of stratigraphic breaks. This indication is an integral component of the event stratigraphy procedure, which we consider essential for assessing the temporal relationships between the carefully studied archaeological sites. Figure 5 displays the levels of horizons with artifacts and radiometric dating of igneous (to the right of the compiled columns) and sedimentary rocks (to the left of the columns).

Igneous analogs of Zanclean (5.3-3.6 Ma), represented by the Cover Basalt Formation [52,88], are the most widely developed in the Eastern Mediterranean. In the Kinneret-Kinnarot troughs, the thickness of the traps of this series in the Zemah-1 borehole reaches 706 m [63]. This is evidence of the highest magmatic activity in the region under study, which undoubtedly influenced the development of ecosystems and the evolution of ancient hominins. The onset of the Piacenzian stage reflects the beginning of the Akchagylian hydrospheric maximum. It was marked by the development of the Erq El-Ahmar lacustrine-alluvial formation in the DST basins (Fig-

ure 2). The rocks of this formation lie on the Cover Basalts and have mainly normal magnetization [89] corresponding to the Gaussian Chron [35]. The subsequent stage of the Akchagylian hydrospheric maximum, with the flooding of the western plateaus by a sea exceeding the current level by 200 m, was marked by the broad development of the Pleshet marine formation in the Mediterranean coastal plain of Israel. This formation underlies continental layers with artifacts and remains of vertebrates in the Evron section [66].

Areal stratigraphic, radiometric, and paleomagnetic analysis

In the stratigraphic subdivision of deposits containing archaeological sites, a rather extensive research methodology is used, associated with the need for ecosystem and historical reconstructions of the habitats of ancient hominin [5,6,69,81]. However, when these sites are correlated even by comparatively accurate physical and chemical methods within the African-Arabian-Caucasian region, modern researchers face complex insoluble problems, both general and regional. This is due to this region's extraordinarily complex geological structure of this region [e.g., 60,65] and the lack of a unified approach to the formation of the Late Cenozoic chronostratigraphic scale. Additional difficulties arise because the paleomagnetic stratigraphy depends on the new data arrival. The manifestation of diverse magmatism, sedimentation diversity, and paleogeographic settings' extreme heterogeneity significantly complicate the regional and basin correlation. Our regional studies have reflected these challenges and ways to overcome them [13]. Therefore, we display the facial analysis using regional tectonic-paleogeographic, chronostratigraphic, radiometric, and paleomagnetic data (Figure 5).

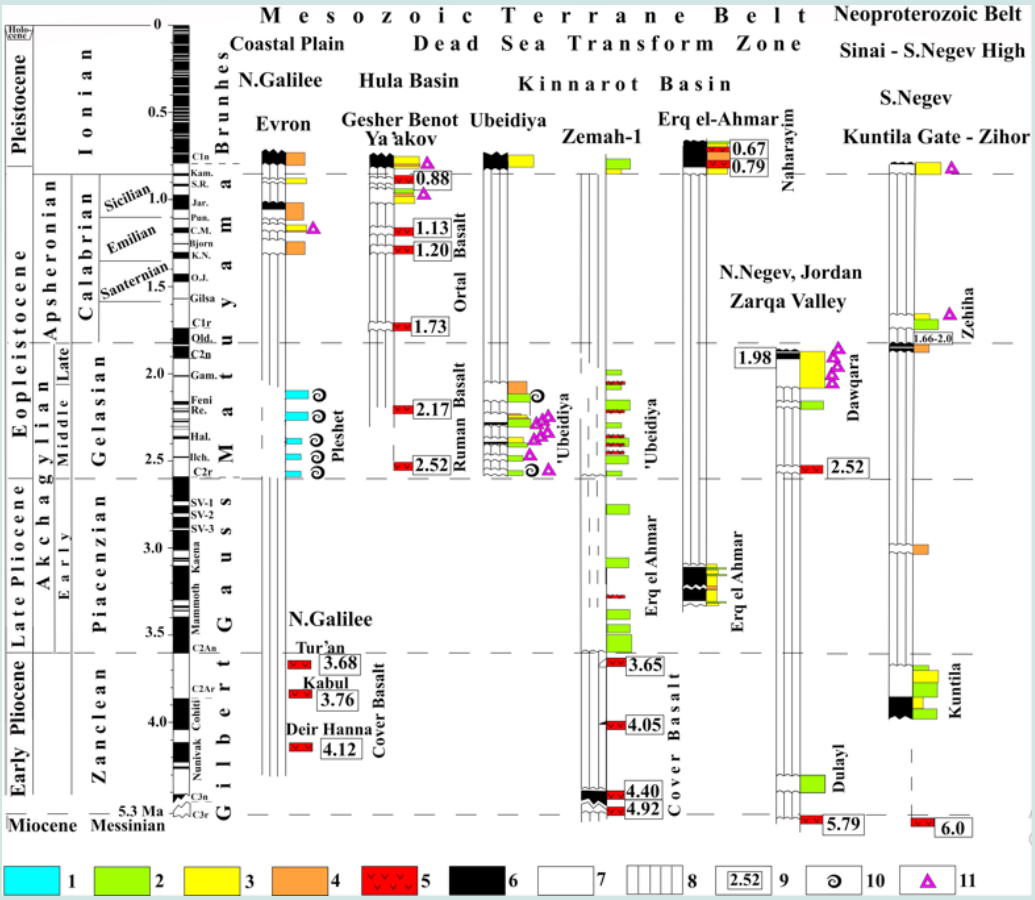

Figure 5: Integrated structural-paleomagnetic-event stratigraphic chart of the northern Levantine ancient hominin sites. (1) marine facies, (2) lake-swamp facies, (3) fluvial facies, (4) soils, (5) basic traps, (6) normal paleomagnetic polarity, (7) reversal paleomagnetic polarity, (8) gaps, (9) radiometric dating, (10) rests of marine benthic fauna, (11) artifacts.
Paleomagnetic subchrons: Kam., Kamikatsura, S.R., Santa Roza, Jar., Jaramillo, Pun., Punaruu, C.M., Cobb Mt., K.N., Kvemo-Natanebi, O.J., Ontong Java, Old, Olduvai, Gam., Gamarri, Re., Reunion, Hal., Halawa, Ilch., Ilchembet (?), SV (1-3), Searles Valley (1-3). The paleomagnetic data were generalized based on [6,21,22,25,27,28,35,36,40–42,66]. The radiometric data were generalized based on [34,36,39, 41,46,47,51,57,63,65,88]. The marine paleontological rests were generalized after [60,67]. The artifacts were generalized after [5,6,41,51,66,70,76,82].
When constructing the chart, the following data for concrete archaeological sites, geological sections and boreholes were used: Evron [4,34,66], Gesher Benot Ya'akov ([34,39,60,77,80], 'Ubeidiya [3,5,6,36,67,78] Erq el-Ahmar [35,36,70,88], Kuntila Gate – Zihor [42,51,60], Zarqa Valley [41], northern Galilee [4,57,73], Zemah-1 well [54,55,60,63].

Table 1 shows the generalization of paleomagnetic, lithological, and archaeological parameters compiled for the first time for the region under study. The parameters for each of the analyzed intervals are analytically summarized at a detailed level. It enabled the substantiation of the paleomagnetic dating scale and indexing of the identified paleomagnetic divisions. Radiometric data and lithofacies characteristics of various layers (trenches) were applied to elaborate the paleomagnetic dating. Besides this, the finds of artifacts separating archaeological sites from sedimentary formations are shown. Analysis of these data indicates a different degree of substantiation of paleomagnetic correlation due to varying details in the sample selection, the heterogeneity of the presented paleomagnetic data nature, the lack of reliable radiometric, biostratigraphic, and lithofacies data, and a comparative analysis of various sections. We have also eliminated significant differences in using the paleomagnetic scale found in publications of different years. Based on this examination, substantiating the paleomagnetic correlation of the given sections looks entirely distinct Table 1.

Table 1

No	Name of site (section)	Index of trench (members)	Artefact presence	Index of specimen	Lithology	Paleomagnetic parameters	Paleomagnetic daring	Reference
1	Evron Quarry	3		e3-1	Red hamra	Axial dipole at 33° N lat.	Brunhes Chron (C1n)	[34,37,66,67,90]
				—		Transition zone	Transition zone	
				e3		Reverse polarity	Latest Matuyama (C1r)	
		4		e4	Sandy yellow-grey gley	Reverse polarity		
			+					
		5		e5-1	Red hamra	Reverse polarity		
				e5-3		ChRM reverse component		
2	Gesher Benot Ya'akov	V		V-4	Clays	Incl. 45-90° N	Earliest Brunhes (C1n) (0.75-0.78 Ma)	[77,80]
			+	V-5	Sands and silts	Incl. 22-60° N		
		I		I-1	Clays	Incl. 44-66° N		
				I-2				
				I-3				
			+	I-4/5				
		II		II-1	Sands	Incl. 15-70° N		
			+	II-2/3				
			+	II-4/5	Sands, silts, and clays			
			+	II-6	Silts	Incl. 30-65° N		
			+	II-7	Silts and clays	Incl. 25-75° N		
		III		III-1	Clays and silts	Incl. 5-55°S	Latest Matuyama (C1r) (0.78-0.786 Ma)	
			+	III-2	Clays and coquina	Incl. 65° S-55° N	Transition zone(0.786-0.8 Ma)	

3	'Ubeidiya	Lu upper limnic member	+	III 56–85, I 33–42, II 43– 1	Upper limnic member with foraminifers	Reverse polarity	Lower Matuyama (C2r)		[2,6,67,76]
		Fi mainly beach deposits	+	III 47–55, I 26–32, II 37–42	Fossil soils and shoreline conglomerates				
				III 34, I 21–25, II 33–36	Fossil soils, fluviatile and littoral deposits				
						Normal polarity		Gamarri event (?)	
			+	III 23–26, I 17–20, II 26–32	Muddy littoral and fossil soils, and shoreline conglomerate	Reverse polarity			
			+						
			+	III 21–22, I 13–15, II 22–25	Muddy littoral and shoreline deposits				
			+			Normal polarity		Feni event (?)	
				II 21	Swampy littoral				
		Li polarity lower limnic member	+	III 4–20 II 2–20	Shallow and deep-water lacustrine sediments with foraminifers	Reverse polarity			
			+						
4	Zarqa Valley	Alluvial fan		S332	Caliche, 1.98±0.2 Ma	VGP lat. 32-85° N	Olduvai subchron (C2n) with the Vrica reversal event		[2,41]
			+		Loam deposits	VGP lat. 40° S VGP lat. 23o N			
				S330	Loam, silt	—	Lower Matuyama subchron (C2r)		
		Shallow gravel-bed river	+		Gravel, silt	VGP lat. 10-67° S			
				S331	Gravel	VGP lat. 20-30° S			
			+	5334 Upp.	Gravel and sands				
						VGP lat. 28-90° S			
				Sukhna	Gravel				
			+	S334 Low.	Slope deposits	VGP lat. 65-85° S			
		Swamp				VGP lat. 40-75° S			
		Upper basalt		B4	Basalt, 2.52±0.01 Ma				
						VGP lat. 80-90° S			
		Flood plain		Dulayl River	Fine sediments with gravels	VGP lat. 14-82° S	Lower Pliocene (subchron C3r)		
						VGP lat. 55° N			
						VGP lat. 2-85° S			
		Lower basalt		Zarqa River	Basalt		Upper Miocene (subchron C3An.1r)		
					5.79±0.01 Ma,	VGP lat. 90° S			
					5.82±0.01 Ma				

5	Erq El-Ahmar	Southern outcrop			Clays, sandstones, conglomerate layer, marls, and limestone			(C2An.4n)	[35,70]
						Incl. 59° N			
						Incl. 10° S		Kaena subchron (C2An.1r)	
		Northern outcrop		pm 38b	Clays, marls, and conglome-rate		Gauss Chron (2An)		
						Incl. 30-60° S			
						Reverse polarity			
				pm 34b	Clays, sands, and conglome-rates				
						Incl. 30-60° N (reverse polarity)		(C2An.5n)	
				pm 20a	Clays with conglomerate layers	Incl. 25-60° N (normal polarity)			
					Soil cover				
				pm 19b	Clays, sands, and marls with conglomerates	Incl. 40-55° N (normal polarity)			
				pm 8a		Incl. 28-60° S (anomalous direction of transition)		Mammoth subchron (C2An.2r)	
6	Kuntila Lake	Sequence 3			Palustrine mudstones and sandstones	VGP lat. 80o S VGP lat. 50o S VGP lat. 77o S	Uncertain polarity		[42,60]
		Sequence 2			Alluvial sandstones and conglomerate	VGP lat. 75o S VGP lat. 78o S VGP lat. 90o S	Gauss Chron (C2An)	Gilbert Chron (C3r, C3n,-C2Ar)	
				KG14-1A					
				KG12-1A					
				KG11-1A	Lacustrine marls, limestone, and sands	VGP lat. 80o N VGP lat. 83o N VGP lat. 20o N VGP lat. 75o N VGP lat. 65-75oN VGP lat. 80o N	Gilbert Chron (C3r, C3n,C2Ar)	Normal polarity subchron C3n	
		Sequence 1		KG5-1A	Distal alluvial mudstones and sandstones				
				KG7-1A	Palustrine and lacustrine mudstones	VGP lat. 75o N VGP lat. 73o N			

Generalization of paleomagnetic parameters observed in the anthropological sites (outcroppings) in the northern part of the Levantine Corridor. It is well-known that the ecostratigraphic nature of deposits is associated with subaqueous and subaerial sedimentation settings. Such a combined analysis, undertaken for the first time as a correlation criterion for the Late Cenozoic sections of the Levant, makes it possible to separate the stages and zones of active sedimentation and the zones and epochs of tectonic-thermal activity that oppose them. These zones and stages reflect the critical phases of the existence and evolution of ancient hominins. Meanwhile, facies and ecostratigraphic analysis of the Levantine sections with artifacts has confirmed the geomorphological and paleogeographical data on alternating stages of hydrospheric disturbances and associated periods of humidification and drying [14].

When correlating the Zarqa (northern Jordan) and 'Ubeidiya (northern Israel) sites (these sites occur in the same paleogeographic zone at a distance of about ~75 km - see Figure 2), we cannot obtain unambiguous data on their geological age. Our studies indicate a low probability that the fluvial lacustrine-bog-alluvial complex with remains of marine foraminifers Ammonia tepida and brackish-water ostracods [67] belonged to Calabrian, the xerophilic stage of post-Gelasian (post-Akchagylian), and the paleomagnetic subchron C1r (Late Matuyama). The probability of their correspondence to the pluvial stage of the Middle-Late Gelasian - Akchagylian and the paleomagnetic subchron C2r-C2n (Early Matuyama) is relatively higher. Event-stratigraphic analysis of the region of the Levantine Corridor indicates that the epochs of moistening and drying are associated with significant hydrospheric disturbances (Figure 4d) (this phenomenon is investigated in detail in [4]. The

development of fluvial rocks with +significant volumes of the remains of the marine fauna inside the DST weakly correlates with the Calabrian regression. The Calabrian stage corresponds mainly to the lower sea level in this region [4,66,90], and discovering marine fauna remains practically rejects this proposition. At the same time, the Akchagylian hydrospheric maximum [7] is mainly associated with the Gelasian stage. Consequently, the 'Ubeidiya section most likely relates to the Gelasian stage.

We cannot reconcile these data with the conclusions about the Acheulean (post-Oldovian) age of the artifacts from the 'Ubeidiya site. Therefore, we propose to apply in this site searching tephrostratigraphic horizons in lacustrine sediments (with subsequent radiometric and paleomagnetic analysis). This technique is justified in the following sections of this article. In the Kinnarot Basin, where are located the essential 'Ubeidiya [6] and Erq El-Ahmar sections [70], the paleomagnetic and radiometric data near the sections and around them are most numerous. The first section contains the 'Ubeidiya Formation (attributed to the upper part of the Matuyama Chron) and the Naharayim Formation, attributed to the Brunhes Chron [6]. The second section contains the Erq El-Ahmar formation (Gauss Chron), 'Ubeidiya formation (Matuyama Chron), and Naharayim formation (Brunhes Chron), separated by stratigraphic breaks (Table 1 and Figure 5). Geochronological, the indicated sections are dated very clearly due to the vast development of effusive and intrusive traps in the DST region. It is studied in detail in the Zemah-1 borehole [54,55]. Cover basalts in this borehole underlie the listed sedimentary formations and diabase sills aged 3.65-4.4 Ma. They correspond to the subchrons C3r, C3n, and C2Ar of the Gilbert Chron (Figure 4b), and these basalt bodies produce numerous magnetic anomalies in the Kinneret and Kinnarot basins [19].

According to radiometric and paleomagnetic data, reliable analogs of Pleshet-Gelasian-Middle Akchagylian are basalts in the Zarqa River (Western Jordan) aged 2.52 Ma [41]. Reversely magnetized bog and alluvial Dawqara Formation, at the top of which caliche is developed [41], overlie them. According to the radiometric data, the latter's age is 1.98 Ma, which corresponds to the Olduvai subchron (C2n). In the upper part of the alluvial complex of this highest terrace of the Dulayl River, remains of large mammals were found: Mammutus meridionalis, Equus cf. tabeti, and Bos primigenius [41]. The Oldowan-like artifacts were identified throughout the terrace section, while the Acheulian tools were found in the younger Birayn Formation of the low terrace [41]. The radiometric and paleomagnetic criteria [41] make it possible to correlate the swarm deposits' thin sequence in the lower part of the Matuyama Chron (see the column 'Zarqa Valley', swamp deposits covering the basalts of 2.52 Ma, in Figure 5).

The Zanclean and Piacenzian deposits in the study area are poorly developed. They are widely developed in the modern shelf of the Mediterranean Sea and the deep-sea basins. Alluvial and lacustrine formations of this age are developed in the DST zone and to the south of it (in the northern part of the Sinai massif). A likely analog of Zanclean is the Dulail Formation (Figure 5) in the eastern Negev terrane of western Jordan (site of Zarqa) (see Figure 2). Here, the lacustrine-marsh formations with reverse magnetization are developed between basalts with an age of 2.52 and 5.79 Ma. They most likely correspond to subchron C3r of the beginning of the Gilbert Chron. It is possible that the same period, judging by the paleomagnetic data and hydrospheric correlation criteria (Figure 4), also corresponds to the Kuntila Formation (Figure 5) of the Paran depression of northern Sinai. There are no anthropological artifacts in these formations. In the section of this formation, an extended zone of the normal polarity is changed to the reverse one [42]. This fact and the absence of artifacts indicate that it most likely corresponds to some interval of the Gilbert Chron. The only artifacts from this area were found northeast - in the Nahal Zihor sites [51]. They belong to the early Lower Paleolithic and are compared with the 'Ubeidiya site [6] and recognized as young Late Acheulean prehistoric tools in younger terraces.

Tectonic-paleomagnetic mapping

Paleomagnetic map of the Hula Basin

The area of the Hula Basin, which includes the northern part of the known sites of ancient hominins (Ma'ayan Baruch, Gesher Benot Ya'akov, 'Ubeidiya, and Erq El-Ahmar), is a depression in the zone of uplifts and troughs of the Dead Sea Transform (DST) (Figures 1 and 2). Tectonically, it is located from west to east between the Upper Galilee's uplifts and the Golan Plateau's northern part. The Korazim Plateau and Mt. Hermon bound it from the south to the north. Tectonic-paleomagnetic mapping displays a very complex pattern of the geological structure distribution (Figure 6). The northern and eastern boundaries of the Hula Basin are limited by Mesozoic and Cenozoic carbonate terrane formations penetrated by dikes and traps of the Jalal paleomagnetic Chron [19]. The southern and eastern parts of the study area are composed mainly of a trap complex of the normal and reverse magnetized rocks of the Sogdiana-2 paleomagnetic Chron (Jalal, Sogdiana, Gissar, Tuarkyr, and Khorezm paleomagnetic classification is described in [91,92]. The oldest components of this Chron, related to the 3n subchron, are developed outside the Korazim uplift. Basalts of the Golan Plateau and the sedimentary complex represent the youngest, associated with the Brunhes Chron 1n, from the Hula Basin.

The most significant is that this region's known sites of ancient hominins are located on the margin of the Hula lake-marsh basin (Figure 2) and received a clear age definition in the outcrop field of the Late Cenozoic trap complex. The ancient site of Gesher Benot Ya'akov [77,80] is in the southeastern corner of the Hula Basin (Figure 1) in the outcrop field of the traps of subchron 1r (Late Matuyama). Their age in this area is 0.9 and 1.73 Ma (Figure 6). According to paleomagnetic data, at this site [77], in a complex of alluvial and soil formations with numerous artifacts, the chrons of Later Matuyama and Early Brunhes are distinguished (Figure 5 and Table 1). The Ma'ayan Barukh site [75] is in the Jordan Valley near the northwestern end of the Hula Basin (Figure 1), in the zone of traps of the paleomagnetic subchron 1r aged 0.89 and 0.93 Ma

(Figure 6). The vast development of trap igneous complexes of 4.5 to 0.12 Ma age in the Hula Basin makes arising sites of the most ancient hominins unlikely here (compared to the more southern regions of the Eastern Mediterranean).

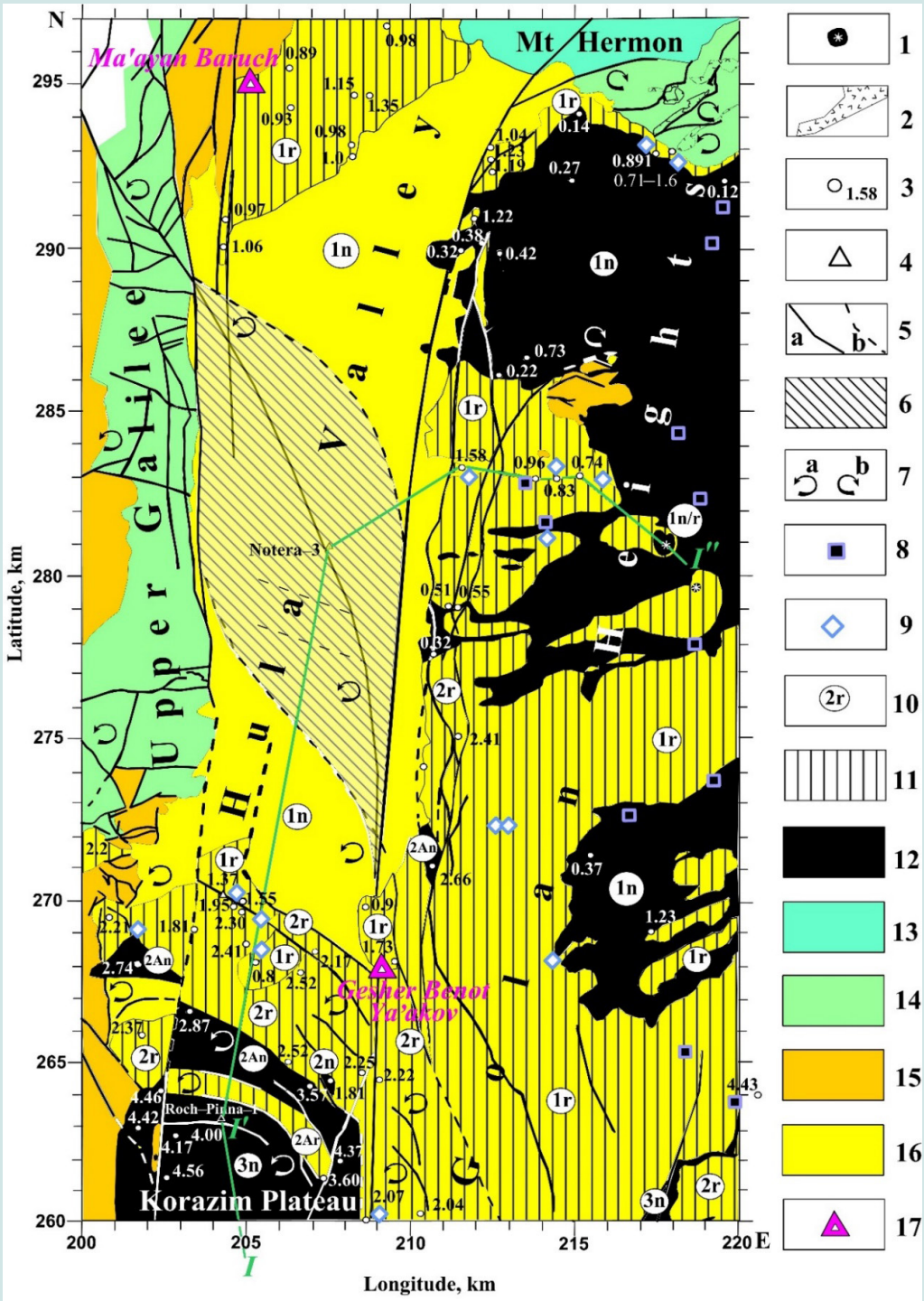

Figure 6: Tectonic-paleomagnetic map of the Hula Basin with the location of ancient hominin sites (location of this area is shown in Figure 1) (based on [14], with supplements).
(1) volcanic cones, (2) Cretaceous traps, (3) outcrops with the radiometric ages of basalts (in Ma), (4) boreholes, (5) faults: (a) observed, (b) reconstructed, (6) pull-apart basin, (7) tectonic blocks rotations: (a) counterclockwise, (b) clockwise, (8) outcrops with the determined normally magnetized basalts, (9) outcrops with the determined reversely magnetized basalts, (10) chrons of the Geomagnetic Polarity Timescale, (11) areas of the reversely magnetized basalts, (12) areas of the normally magnetized basalts, (13) Gissar superzone, (14) Jalal superzone, (15) Tuarkyr – Khorezm superzone, (16) Sogdiana superzone, (17) ancient hominin site. Tectonic setting after [34,45,56,61,71]. Radiometric data (K-Ar and Ar-Ar) after [34,46,49,50,57].

Paleomagnetic map of Lake Kinneret

Located south of the Hula Basin, the more extensive and intensively submerged Kinneret-Kinnarot Basin (Figure 1) extends south to the Dead Sea. It is underlain by a powerful salt-bearing Miocene sequence [51]. According to paleomagnetic mapping data, the older basaltic series of the zone Sogdiana-2 dominate (Figure 7). Their radiometric age ranges from 17.7 to predominantly 3-4 Ma, corresponding to the 5Cr - 3n subchrons of the standard Miocene-Pliocene magnetostratigraphic scale. The most extensive outcrop area is subchron 3n, developed in the Lower Galilee and the Korazim Plateau, and subchron 3r outcropping on the Golan Plateau and partly to the west of the DST. Many authors note the extremal complex tectonic mosaic structure of this area [16,19,34,56,57,60,63].

Magnetic data analysis indicates that the subchrons 3r and 3n mentioned above comprise the Kinneret-Kinnarot basins throughout [19] and correlate well with the adjacent 3n and 3r subchrons in the Golan Plateau and the Lower Galilee (Figure 7). Sedimentary formations of the Pliocene-Pleistocene of the Kinneret-Kinnarot Basin have been studied in boreholes and natural outcrops. These formations compose the Erq El-Ahmar, 'Ubeidiya, Naharayim, and Lisan formations and younger alluvial, lacustrine, and soil complexes of Holocene formations. They are partially dated by paleomagnetic and radiometric data [35,36,47]. According to the analysis of cores from the Zemah-1 well [55], the thickness of these formations reaches 500 m. Following the study of seismic profiling data and structural mapping data, the thickness of these formations reaches 1750-2000 m [89], which indicates the significant tectonic subsidence of the central zone of the pull-apart basin. The outcrops of the Lisan, 'Ubeidiya, and Erq El-Ahmar formations are known on the sides of the DST at elevations from -200 to -100 m. In the Kinneret-Kinnarot basin itself, judging by magnetic, seismic data analysis and subsequent structural mapping, Pliocene and Pleistocene sedimentary formations have undergone significant deformation. This peculiarity must be considered in studies of paleomagnetic strata stratigraphy that include archaeological objects.

According to the available data [35], the Erq El-Ahmar Formation is characterized mainly by normal polarity and most likely corresponds to the Gaussian Chron 2An and correlates with the Lower Akchagylian (Piacenzian). The 'Ubeidiya Formation has predominantly reverse polarity [6,44] and corresponds to the Matuyama Chron (Table 1 and Figure 5). According to the available data (Figure 4b), the upper half of the above chron is characterized by more widely developed intervals of normal magnetization, not to mention the development in the middle part of the Olduvai C2n subchron with a duration of about 0.15 Ma. Therefore, the 'Ubeidiya Formation most likely corresponds to a predominantly reversely magnetized lower part of the Matuyama Chron C2r (Figures 4b and 5), similar to the Dawqara formation of Jordan, well mapped by paleomagnetic and radiometric methods and containing artifacts and remains of ancient mammals [41].

This map also indicates that lacustrine-alluvial basins inside the DST have been formed on basaltic trap fields after Earlier Pliocene (Zanclian). Beginning in the Later Pliocene, south of the Korazim Plateau, in the Sea of Galilee and Kinnarot Basin areas (Figure 7), ecosystems favorable for humanoid habitation were formed. The paleomagnetic mapping examination and analysis of the trap occurrence and sedimentary complexes indicate that the Upper Cenozoic formations are significantly lowered in the DST strip. Their initial formation level could differ from modern by 200-300 m. This circumstance can explain the findings of marine foraminifers in the lacustrine sediments of the 'Ubeidiya site and Mazar section [67]. It is essential that Hall et al. [60] interpret the Mazar 6m thick section (which is located at 60m altitude) as a marginal marine intercalation within the Arava Formation (in the DST zone). They were widely developed in the nearby sea bays of the Akchagylian-Gelasian high transgression series. Moreover, the assumption that the 'Ubeidiya Formation belongs to the Calabrian stage (the second half of the Matuyama Chron) (Figure 4b) does not coincide with several geological criteria since just sediments of the Gelasian stage have been formed during the transgressive phase and significant subsidence of the DST pull-apart basins.

Paleomagnetic profile 'Kinnarot Valley - Lake Kinneret - Hula Basin'

Paleomagnetic profiling is an essential tectonic-geodynamic component for paleomagnetic mapping [12]. The paleomagnetic profile along the DST system of uplifts and troughs (Figure 8) is drawn through a series of heterogeneous structures of the Mesozoic Terrane Belt [19,62] to the marginal part of the Neoproterozoic Belt (Figure 2). Numerous studies have shown that in this region, both classical shear structures (pull-apart basins) and heterogeneous ring rotation structures are developed [e.g., 16,19,33,34,47,52,58,59,63]. These structures were generalized in the paleomagnetic profile (Figure 8).

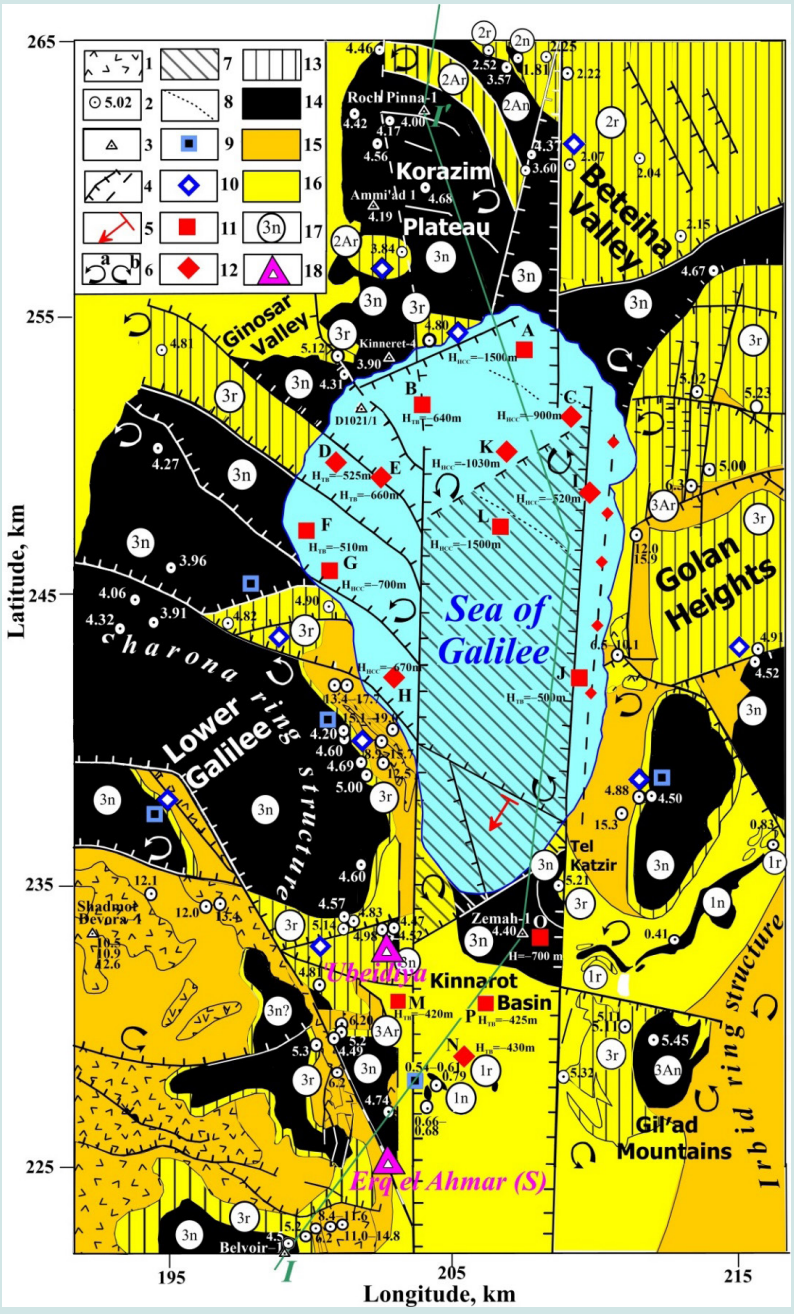

Figure 7: Integrated tectonic paleomagnetic scheme of the Lake Kinneret (Sea of Galilee) (location of this area is shown in Figure 1) (based on [19], with supplements).

(1) outcropped Cenozoic basalts, (2) points with radiometric age of basalts (in m.y.), (3) boreholes, (4) faults, (5) general direction of the proposed buried basaltic plate dipping in the southern part of the Sea of Galilee, (6) counterclockwise (a) and clockwise (b) rotation of faults and tectonic blocks, (7) pull-apart basin of the Sea of Galilee, (8) suggested boundaries of the paleomagnetic zones in the sea, data of land paleomagnetic measurements (9 and 10): (9) normal magnetization, (10) reverse magnetization, (11 and 12) results of magnetic anomalies analysis: (11) normal magnetization, (12) reverse magnetization, (13) reversely magnetized basalt fields, (14) normal magnetized basalt fields, (15) Miocene basalts and sediments with complicated paleomagnetic characteristics, (16) Pliocene-Pleistocene basalts and sediments with complicated paleomagnetic characteristics, (17) index of paleomagnetic zonation, (18) ancient hominin sites.

Tectonic setting after [34,58,59,71]. 1n, 2n, 3n, 1Ar, 2Ar, and 3Ar are the indexes of paleomagnetic zones [16]. Radiometric data (K-Ar and Ar-Ar) after [33,34,36,47,57,63]. Paleomagnetic data after [32,34,36,38,40,46,47,53]. HTB and HHCC designate calculated depths of basaltic bodies in the basin: HTB is the upper edge for the model of a thin bed, HTHP is the upper edge for the model of a thin horizontal plate, and HHCC is the center for the model of a horizontal circular cylinder. The bold green line shows the location of paleomagnetic profile *I* – *I'*.

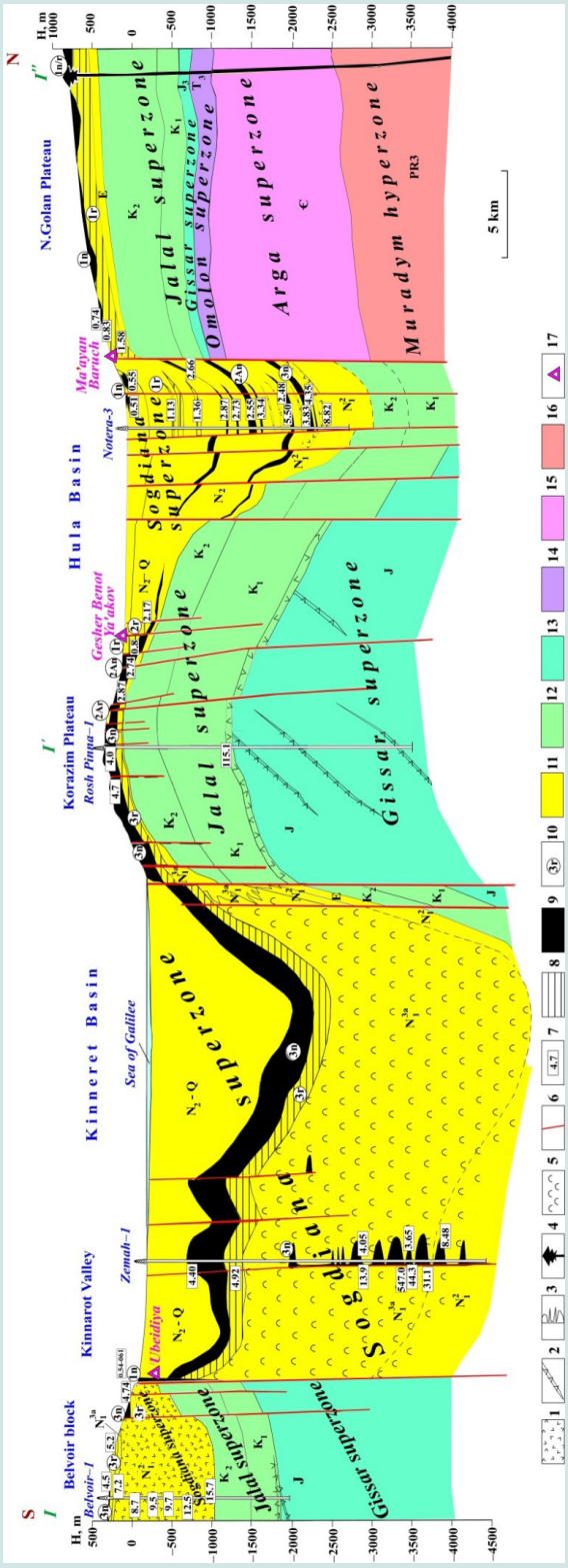

Figure 8: Paleomagnetic profile Kinnarot Valley – Lake Kinneret – Hula Valley (its location is shown in Figure 1) (based on [19], with supplements).

(1) basic traps, (2) basic dykes, (3) gabbro, (4) volcanic cones, (5) evaporite sediments, (6) faults, (7) radiometric dating, (8) reversal polarity, (9) normal polarity, (10) indexes of Pliocene-Pleistocene magnetostratigraphic scale, (11) Sogdiana superzone, (12) Jalal superzone, (13) Gissar superzone, (14) Omolon hyperzone, (15) Arga hyperzone, (16) Moradym hyperzone, (17) ancient hominin site. The primary utilized sources (besides publications presented in the captions for Figures 6 and 7) are [19,63].

On the paleomagnetic profile in the left shear zone of the Antilebanon terrane (Belvoir block), a thick zone of Miocene traps is traced, associated with the boundary of the Sharona ring structure (contoured in Figure 7). To the northeast, along the profile line, this block abruptly gives way to the Kinneret-Kinnarot trough filled with a thick layer of the Early Messinian salt, the Pliocene Cover Basalts, and the terrigenous alluvial-lacustrine Pliocene-Quaternary formations. All the mentioned rocks are combined into a unified Sogdiana-2 paleomagnetic superzone. Geodynamically, this extremely active superzone is intruded by Pliocene gabbroids aged about 3.65-4.05 Ma, among which older igneous formations of the Miocene (13.9 Ma), Oligocene (31.1 Ma), Upper Eocene (44.3 Ma), and even Cambrian (547 Ma) are developed [63]. A thick salt layer is an analog of the tectonic-compensation mechanism of regressive half-rhythms filling a deep trough under a short-term transgressive inflow. This salt-bearing stratum is similar to the Bira and Gesher formations - carbonate sediments occurring near Galilee Plateau and Golan Heights [4,57,72,73,74]. This transgressive sequence corresponds to the Early Messinian, an analog of the Pontian stage of the Paratethys Basin. On the southwestern coast of the Sea of Galilee, a set of foraminifer remains (Ammonia beccarii and Elphidium sp.) was recognized [60]. It formed a hydrospheric maximum similar to the Akchagylian-Gelasian (Figure 4d). In the area of the Hula Basin, this maximum did not manifest itself due to the isolation of the DST studied part from the central bay. Thus, the paleomagnetic profile visibly shows two hydrospheric maxima, Pontian and Akchagylian (Figure 4d), and recognized marine Ammonia foraminifers [67], manifested their development in the same northern part of the DST zone. In light of these data, the 'Ubeidiya site is likely to correspond not to the regressive Calabrian but to the Gelasian stage.

Development of the map of palinspastic reconstructions

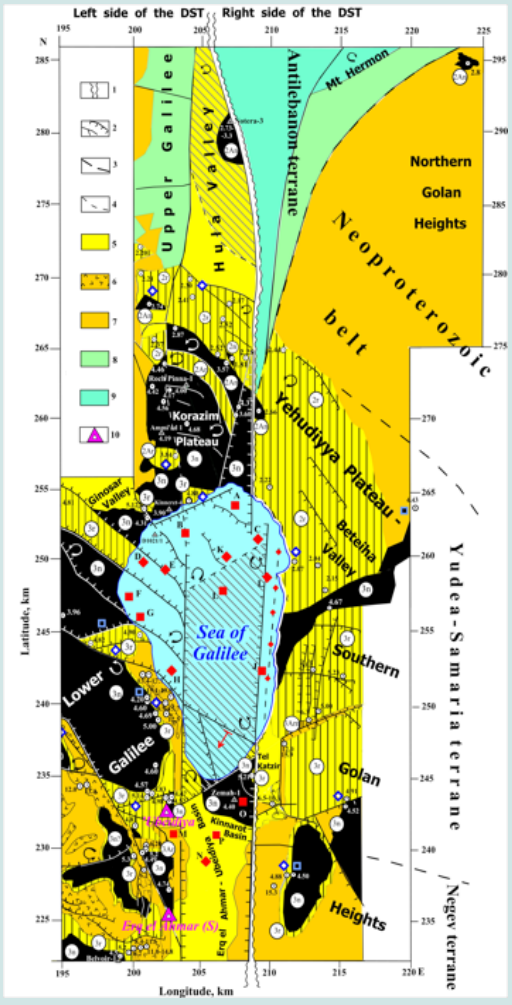

Figure 9: Tectonic-paleomagnetic palinspastic map of the Sea of Galilee – Hula region for the period of 3.6 – 2.0 Ma. (1) area of joining of the left and right DST blocks on the palinspastic reconstruction, (2) faults, (3) boundaries of terranes, (4) marginal boundaries of the pull-apart basins, (5) Post-Miocene Cover Basalts - Ruman basalts of the Sogdiana superzone (upper part), (6) Miocene basalts of the Sogdiana superzone (middle part), (7) Tuarkyr-Khorezm superzone, (8) Jalal superzone, (9) Gissar superzone, (10) paleomagnetically investigated outcrops of the Gauss-Matuyama Chrons (2An-2r ?) in the DST fluvial facies. Other designations are in Figure 7.

Many years of tectonic-geodynamic experience in northern Israel showed that magnetostratigraphic elements' structural and temporal analysis is not sufficiently investigated due to significant displacements of tectonic blocks. The composed paleomagnetic maps (Figures 6 & 7) and paleomagnetic profile (Figure 8) were used for the development of the map of palinspastic reconstruction (for the period of 3.6 - 2.0 Ma) in the Hula - Sea of Galilee - Kinnarot basins and framing uplifts of the DST (Figure 9). Such a map sheds light on the tectonic-magmatic evolution of the 'Ubeidiya anthropological site and references the Erq el-Ahmar section.One of the fundamental problems here is the geological imagination of the displacement amplitude. According to regional data, the total amplitude of the shear zone is 100 km [60]. At the same time, the activation (movement) time, derived from the radiometric and geodynamic data, is 20 Ma [93]. Thus, the eastern side of the DST moved along the left after the end of the Akchagylian hydrospheric-geodynamic maximum (~2.0 Ma) [7] strike-slip to the north by about 10 km.

An essential element of the paleomagnetic-geochronological reconstruction is the reduction of young trap and sedimentary complexes that formed 3.6 - 2.0 Ma mainly in the east, the northern part of the Golan Plateau, and partly in the Hula and Kinnarot basins. Paleomagnetic investigation of traps in the Sea of Galilee area is complemented by magnetostratigraphic data from examining sedimentary rocks in the Jordan Basin, where the lacustrine-alluvial complexes of the Erq el-Ahmar and 'Ubeidiya formations (Figure 9) are developed. These formations mainly relate to the Gauss and Matuyama Chrons, respectively. The traps of the zone of the lower part of the Matuyama Chron (C2r) are widely developed on the Yehudiyya Plateau and in the transition zone of the Korazim Plateau and the Hula Basin (Figure 9). Post-cover basalt traps - Eitar Basalts (2.6-3.6 Ma) and Ruman Basalts (2.04-2.52 Ma) correspond to the lower and middle Akchagylian and, according to palinspastic mapping, are characterized by a reasonably compact occurrence.

Subchron C2An (Gauss Chron) is developed on the northern slope of the Korazim Plateau and, to a lesser extent, in the pull-apart basin of the Hula Basin, and on the northernmost slope of the carbonate platform of the Neoproterozoic belt, at the boundary with the Hermon terrane (Figure 9). Thick traps of the Northern Golan Plateau (Ortal Basalts - 1.8-0.89 Ma and Golan Basalts - 0-0.85 Ma), comparable to the Miocene basalts of Galilee, are missing from a palinspastic reconstruction compiled for an older epoch (> 2 Ma). This map shows (Figure 9) that the alluvial-lacustrine deposits of the Erq El-Ahmar and 'Ubeidiya formations correspond to the radiometrically and paleomagnetically dated trap complexes of 3.6-2.0 Ma and relate to subchrons 2An - 2r (Gauss and Lower Matuyama Chrons). This confirms our earlier assumption that 'Ubeidiya Formation belongs to the Gelasian stage.

This palinspastic reconstruction (Figure 9) is essential for the paleogeographic assessment of the unique lacustrine-alluvial basin Erq El-Ahmar - 'Ubeidiya as a landscape optimum for the habitat of ancient hominids, relatively isolated from the surrounding uplifts. Tectonically, this basin coincides with two DST troughs,

a. The pull-apart basin of the present-day Sea of Galilee and

b. The narrower southward elongated Kinnarot trough.

This relatively long-lived (more than 1 million years) lacustrine-alluvial submeridional basin was limited from the west and east by complexly dislocated tectonic blocks of the uplifts of the Lower Galilee and the southern part of the Golan plateau. A thick series of Miocene traps and Early Pliocene Cover Basalts cover these blocks. They show that the stage of formation of the pluvial lacustrine-marsh-alluvial basin Erq El-Ahmar - 'Ubeidiya in tectonic-paleogeographical terms differs sharply from the previous one - the Miocene-Early Pliocene stage, during which active trap volcanism and differentiated tectonic movements developed [47,57]. The palinspastic reconstruction reveals another important circumstance explaining the settlement of ancient hominids from the Levant region. It relates to the fact that from the north, the basin 'Ubeidiya - Erq El-Ahmar was limited by the most significant zone of the Antilebanon uplift, the Northern Golan plateau, the uplift of the Upper Galilee, the Korazim and Yehudiyya plateaus. This fact shows that in the north, landscape conditions were unfavorable for the settlement of the ancient hominids of the Levant in the regions of Eurasia. At the site of this uplift, the trap volcanism of the Korazim, Yehudiyya, and Hula Valley plateaus was also developed, which have a paleomagnetic age of C2Ar-C2r, supplemented by radiometric dates from 3.6 to 2.04 Ma (Figure 9).

The map shows that the 'Ubeidiya and Erq El-Ahmar formations form a single tectonic-paleomagnetic and belong to a continuous paleogeographic pluvial cycle of the Gauss - Lower Matuyama paleomagnetic Chrons. Geologically and paleomagnetically, the assignment of the 'Ubeidiya Formation to the Upper Matuyama Chron of 1.6-1.2 Ma [6] is unacceptable since a significant geological break at the boundary of the Gauss and Matuyama Chrons is not confirmed cartographically. Moreover, according to paleomagnetic data, the Lower Matuyama Chron corresponds to the beginning of the tectonic subsidence of the region, which can be seen from the vast Yehudiyya Plateau and the northern edge of the Korazim Plateau (Figure 9). Thus, the tectonic-paleomagnetic palinspastic reconstruction indicates that the 'Ubeidiya Formation belongs to the Lower Matuyama Chron (2.6-1.9 Ma) [94]. The palinspastic map (Figure 9) demonstrates that this conclusion should be verified based on the search for ash complexes and a fragment of igneous rocks in the 'Ubeidiya Formation, followed by their radiometric dating since the traps of Gelasian analogs (2.0-2.6 Ma) are located 12-15 km northeast of the 'Ubeidiya section. This conclusion was obtained earlier with the detailed paleomagnetic mapping of the study area. The utilized sources are presented in captions to Figures 6-8.

Discussion

In such geologically complex regions as the Levantine Corridor, the application of single Earth Science methods, as a rule, is

ineffective. As shown in Section 2.3, combining different methods hardly decreases the probability of incorrect solutions. Therefore, we analyzed an integrated geological-geophysical data set for the region under study. According to radiometric data, the Zarqa Valley complex in Jordan (2.52-1.98 Ma) (Figure 5) is considered the most ancient site in the Eastern Mediterranean. The 'Ubeidiya site is dated with the younger formations. Meanwhile, the 'Ubeidiya and the Zarqa sections require a mutual evaluation based on analyzing the completeness of the presented deposits and the set of structural and facial complexes, archaeological sites, and a complex of organic remains characteristic of various paleoecological associations. The data of tectonic-sedimentary analysis indicate that the 'Ubeidiya and Erq El-Ahmar sections are areas of depression facies of the lacustrine-swampy, estuary, and alluvial-delta series, confined to troughs of the DST shear zone and its diagonal branches. This circumstance is essential for analyzing the completeness of the section and event-stratigraphic correlations. The section of the Zarqa River Valley is, concerning the DST strike-slip regional trough, a zone of uplifted marginal horst, which belongs to the strike-slip block of the Negev terrane, is displaced to the north by 100 km relative to the DST. Highly elevated river terraces are developed here, connected with a hydrographic network incised into the uplands of the Arabian lithospheric plate. This was a typical landscape of this tectonic region for the latest Cenozoic, where ecosystems were not optimal and diverse under arid plateaus.

El Zaatari [79] indicates that on the SW coast of Lebanon, near the city of Saida, on the northernmost boundary of our paleogeographic map (Figure 1), there is the Lower Paleolithic site of Borj Qinnarit, overlying a sea terrace of 95 m altitude. A pebble culture represents artifacts in the overlying site without bifaces. The author notes that the dating of this terrace corresponds to the isotopic stage 16-17, relating to 650 kyr. The continental formations may be more ancient, corresponding to the structural terrace of Piacentian - Gelasian, widely developed to the south, on Mt. Carmel, and in Galilee [19]. Younger sites with the Acheulean lithic industry are developed north of the study area, in Beirut district. They lie at lower hypsometric marks [79], corresponding to the Israeli Early Paleolithic Evron site [4]. These data require careful study using rhythm-stratigraphic, biostratigraphic, and paleomagnetic data. However, future studies are proposed to significantly expand the data on the distribution of ancient hominin sites in the Levant, which are currently known as single objects.

The analysis of paleogeographic data (Figure 2) indicates why there are no analogs of the site from the section of the Zarqa River terrace at the end of Gelasian-Akchagylian in the Kinneret-Kinnarot area. Not only the Late Akchagylian sea level drop by ~ 200 m, but also the climate aridization likely causes it. The main reason is that at the same time, trap magmatism sharply increases north of Lake Kinneret and the Korazim plateau. Volcanism sharply increases here, covering vast expanses north of the Golan Plateau. The ancient community dispersals from the draining estuary of the Kinneret-Kinnarot to the southeast to the river valleys running down from the heights of the Arabian Plate to the area of the shifted Negev block where the carbonate platform is characterized by the optimal landscape and climatic conditions. Here, aquifers of the Triassic and Jurassic are developed, and there are favorable soil and plant ecosystems, in contrast to the Cretaceous stony deserts.

The developed paleomagnetic maps and profile (Figures 6-8) contributed to identifying tectonostratigraphic features of the northern part of the Levantine Corridor and made it possible to clarify the age of the 'Ubeidiya anthropological site. Paleomagnetic mapping and profiling (Figures 6-8) allow using the basin correlation criterion to analyze the sediments containing archaeological sites. Of most significant interest is the Kinneret-Kinnarot sedimentary basin, bounded by trap plateaus: Korazim in the north, Lower Galilee in the west, and Golan Heights and Gil'ad Mts. in the east (Figure 7). Sites Erq El-Ahmar (Gauss zone) and 'Ubeidiya (Matuyama zone) are located near the southwestern end of the pull-apart basin. They combine two sedimentation cycles of lacustrine-fluvial deposits and lie on the Cover Basalts (Gilbert zone) traps corresponding to the Zanclean Stage of the Lower Pliocene (Figures 4 & 8). Significant stratigraphic breaks exist between the traps and sedimentary rocks and within the sedimentary formations (Figure 5). As seen in Figure 7, the rhomb-shaped pull-apart basin extends in a diagonal direction onto the slopes of the adjacent uplifts from the area of the 'Ubeidiya site to the Beteiha Valley. At the same time, the general stage of subsidence of the basin is marked, as it were, containing basalt traps in the northeast, dated from 2.25 to 2.04 Ma, corresponding to subchron 2r (Early Matuyama).

It is important to note that to the north of the elevated southern part of the Golan Plateau, covered by the Early Pliocene Cover Basalts subchrons 3n and 3r aged 5.23-4.50 Ma, and there is a much younger Beteiha Valley structure. It comprises alluvial rocks and basalts aged 2.25-2.04 Ma, corresponding to the C2r (Lower Matuyama paleomagnetic subchron). The same formations can be traced on the Korazim Plateau's northern flank and the Hula Basin's eastern coast (Figures 6 & 7). According to the basalts' radiometric dating in the Notera-3 borehole (Figure 8), only subchrons 3n, 2An, and C1r (Gauss Chron and Upper Matuyama subchron) are developed in the basin itself. The subchron C2r (Lower Matuyama), typical for the Lake Kinneret region, the Kinnarot trough, and the Beteiha diagonal depression, is not developed.

In this work, we have undertaken a complex method of paleogeographic, paleomagnetic mapping, event stratigraphy, and cyclical analysis, during which the place of the 'Ubeidiya site and other objects close to it have become probabilistic in the regional geological scale of the Eastern Mediterranean. The palinspastic reconstruction (Figure 9) has been performed corresponding to the stage of the most significant tectonic-hydrospheric disturbances (3.6 - 2.0 Ma). It indicates how, at a new research stage, quantitative age data for the 'Ubeidiya site can be obtained based on the correlation of sedimentary formations (with the search for tephrostratigraphic correlatives) and closely spaced radiometrically and paleomagnetically studied trap complexes [94]. Syn-sedimentation

basin correlation is a significant factor in determining the age of the 'Ubeidiya formation. However, this correlation must be verified by examining the section of this site itself. It is undoubtedly necessary to carry out detailed sedimentological surveys to search for traces of volcanic ash and the remains of traps of different ages (that have undergone erosion and transfer) with their subsequent radiometric dating. The detailed paleomagnetic interpretation of the volcanogenic-sedimentary complexes containing unique archaeological sites prompts the use of novel aspects for their age analysis.

The 'Ubeidiya stratotype, on the other hand, reflects a vast optimal zone of diverse ecosystems, both subaqueous and subaerial, which developed over a very long time, judging by the cyclic alternation of lacustrine, coastal, and terrestrial facies. The section is composed mainly of lacustrine and coastal-fluvial, primarily carbonate formations of considerable thickness with numerous remains of terrestrial and aquatic organisms and with horizons developed throughout the section with an archaic stone industry of the Oldowanian-Early Acheulean type [76]. Among the remains of large mammals were identified: Mammutus meridionalis, Ursus etruscus, Equus tabeti, Stephanorhynus etruscus etruscus, Kolpochoerus olduvaaiensis, Panthera gombaszoegensis, Macaca sylvanus, and some others [5,6]. However, the dating of these paleontological remains is very complex and beyond the scope of our study.

It is essential that in the basal part and the top of the 'Ubeidiya Lake sequence, marine foraminifers Ammonia tepida that can inhabit brackish water basins were found [67]. This is clear evidence of a connection between the 'Ubeidiya estuary and the transgressive Pleshet basins (see Figure 5) located to the west within the carbonate plateau of Galilee, whose height, according to our studies, exceeded the current sea level by 100-200 m. Paleomagnetic data confirm this conclusion, i.e., the dominant reverse polarity of deposits in the 'Ubeidiya section with two thin subchrons of normal polarity in the middle part of the section [5]. This situation is more consistent with the lower half of the Matuyama Chron (2.6-2.0 Ma interval) (Figure 4b), where, according to a thorough study of the East African trap complex [30], a sign-alternating interval was revealed. In the upper part of the Matuyama Chron, subchrons of the normal polarity of Ontong Java, Kvemo-Natanebi, and Cobb Mt. in the interval of 1.6-1.2 Ma (Figure 4b) had a more extended character. In addition, in the DST depression zone, the presence of the Calabrian regressive Matuyama Chron (instead of the transgressive Gelasian) seems unlikely.

This correlation also follows from the data from the Evron section, where the Late Matuyama Chron with an extensive Jaramillo subchron [37] and a different character of artifacts and a complex of large mammals is developed in the section of continental dominant, red-colored formations [66]. It geochronologically corresponds to the 1.3-0.9 Ma stage. Thus, the supposedly relative age of the Calabrian 'Ubeidiya Formation (1.6-1.2 Ma) can be revised. This age does not correspond to the extensive data available from climatostratigraphic, magnetochronological, and paleogeographic studies concerning sea and river terraces, analysis of hydrospheric disturbances, and related climatic epochs, which manifest themselves in the alternation of vast arid and humid zones.

References

1. Fleagle JG, JJ Shea, FE Grine, AL Baden, RE Leakey (2010) An Ecological Perspective. Out of Africa I: The First Hominin Colonization of Eurasia, Vertebrate Paleobiology and Paleoanthropology. Sourcebook of Paleolithic Transitions, Springer, Dordrecht, pp. 304-310.
2. Enzel Y, O Bar-Yosef (2017) Quaternary of the Levant. Environments, Climate Change and Humans. Cambridge University Press, Cambridge, UK pp. 771-775.
3. Barash A, M Belmaker, M Bastir, M Soudack, DHD Oaley, et al. (2022) The earliest Pleistocene record of a largest Pleistocene from the Levant supports two out-of-Africa dispersal events. Scientific Reports 12(1721): 1-10.
4. Eppelbaum, LV, YI Katz (2022) Combined Zonation of the African-Levantine-Caucasian Areal of Ancient Hominin: Review and Integrated Analysis of Paleogeographical, Stratigraphic and Geophysical-Geodynamical Data. Geosciences (Switzerland) 27(1): 1-23.
5. Bar-Yosef O, M Belmaker (2011) Early and Middle Pleistocene faunal and hominins dispersals through Southwestern Asia. Quaternary Science Reviews 30(11-12): 1281-1295.
6. Bar-Yosef O, M Belmaker (2017) Ubeidiya. In: (Enzel Y & Bar Yosef Y, Eds), Quaternary of the Levant, Part III: Archaeology of Human Evolution, Cambridge University Press pp. 179-186.
7. Eppelbaum, L, Yu Katz (2021) Akchagylian Hydrospheric Phenomenon in Aspects of Deep Geodynamics. Stratigraphy and Sedimentation of Oil-Gas Basins No 2(1): 8-26.
8. Lapkin IY, YI Katz (1990) Geological events at the Carboniferous and Permian boundary. International Geology Review 32(9): 853-866.
9. Eppelbaum LV (2010) Archaeological geophysics in Israel: Past, Present and Future. Advances in Geosciences 24(1): 45-68.
10. Eppelbaum LV (2015) Quantitative interpretation of magnetic anomalies from thick bed, horizontal plate and intermediate models under complex physical-geological environments in archaeological prospection. Archaeological Prospection 23(2): 255-268.
11. Eppelbaum LV, YI Katz (2015) Newly Developed Paleomagnetic Map of the Easternmost Mediterranean Unmasks Geodynamic History of this Region. Central European Jour. of Geosciences (Open Geosciences) 7(1): 95-117.
12. Eppelbaum LV, YI Katz (2015) Paleomagnetic Mapping in Various Areas of the Easternmost Mediterranean Based on an Integrated Geological-Geophysical Analysis. In (Eppelbaum L, Ed.), New Developments in Paleomagnetism Research, Ser: Earth Sciences in the 21st Century. Nova Science Publisher, New York, United States pp. 15-52.
13. Eppelbaum LV, YI Katz (2021) Deep Tectono-Geodynamic Aspects of Development of the Nubian-Arabian Region. In: The Arabian Seas Biodiversity, Environment Challenges and Conservation Measures (Ed L Jawad), Springer pp. 199-237.
14. Eppelbaum LV, YI Katz (2022) Paleomagnetic-geodynamic mapping of the transition zone from ocean to the continent: A review. Applied Sciences 12(1): 1-20.
15. Eppelbaum LV, BE Khesin, SE Itkis (2001) Prompt magnetic investigations of archaeological remains in areas of infrastructure development: Israeli experience. Archaeological Prospection 8(3): 163-185.
16. Eppelbaum L, Z Ben-Avraham, Y Katz, S Marco (2004) Sea of Galilee: Comprehensive analysis of magnetic anomalies. Israel Jour. of Earth Sciences 53(3): 151-171.
17. Eppelbaum LV, Z Ben-Avraham, YI Katz (2007) Structure of the Sea of Galilee and Kinarot Valley derived from combined geological-geophysical analysis. First Break 25(1): 21-28.

18. Eppelbaum LV, BE Khesin, SE Itkis (2010) Archaeological geophysics in arid environments: Examples from Israel. Journal of Arid Environments 74(7): 849-860.

19. Eppelbaum, LV, YI Katz, Z Ben-Avraham (2022) Advanced combined geophysical-geological mapping of the Sea of Galilee and its vicinity. In: (Eds: A di Mauro, A Scozzari, S Soldovieri) "Instrumentation and Measurement Technologies for Water Cycle Management", Springer pp. 141-179.

20. Liddicoat JC, ND Opdyke, GI Smith (1980) Paleomagnetic polarity in 930-m core from Searles Valley, California. Nature 286(1): 22-25.

21. Grishanov AI, VN Eremin, ZA Imnadze, TG Kitovani, ShK Kitovani, et al. (1983) Stratigraphy of the Upper Pliocene and Upper Pleistocene deposits of Guria (Western Georgia) based on paleontological and paleomagnetic data. Bull. of the Committee for the Study of Quaternary period. (In Russian) Nauka, Moscow pp. 18-28.

22. Tretyak AN, LI Vigilyanskaya, VN Makarenko, VP Dudkin (1989) Fine structure of the Geomagnetic Field in the Late Cenozoic. (In Russian) Naukova Dumka, Kiev, Ukraine pp. 155-165.

23. Walter RC, PC Manega, RL Hay, RE Drake, GH Curtis (1991) Laser-fusion 40Ar/39Ar dating of Bed I, Olduvai Gorge, Tanzania. Nature 354(1): 145-149.

24. Berggren WA, Hilgen FJ, CG Langereis, DV Kent, JD Obradovich, et al. (1995) Late Neogene chronology: New perspectives in high resolution stratigraphy. GSA Bulletin 107(11): 1272-1287.

25. Cande SC, DV Kent (1995) Revisited calibration of the geomagnetic polarity timescale for the Late Cretaceous and Cenozoic. Journal of Geophysical Research 100(4): 6095-6095.

26. Pouliquen G, Y Gallet, P Patriat (2001) A geomagnetic record over the last 3.5 million years from deep-low magnetic anomaly profiles across the Central Indian Ridge. Journal of Geophysical Research 106(B6): 10,941-10,960.

27. Cohen KM, PL Gibbard (2019) Global chronostratigraphical correlation table for the last 2.7 million years, version 2019 QI-500. Quaternary International 500(1): 20-31.

28. Channell JET, BS Singer, BR Jicha (2020) Timing of Quaternary geomagnetic reversals and excursions in volcanic and sedimentary archives. Quaternary Science Reviews 228(1): 1-29.

29. Roger S, C Coulon, N Thouveny, G Feraud, A Van Velzen, et al. (2000) 40Ar/39Ar dating of a tephra layer in the Pliocene Seneze maar lacustrine sequences (French Massif Central): constraint on the age of reunion-Matuyama transition and implications on paleoenvironmental archives. Earth and Planetary Science Lett 183(3-4): 431-440.

30. Deino AL, C Heil, CJ King, LJ McHenry, IG Stanistreet, et al. (2021) Chronostratigraphy and age modeling of Pleistocene drill cores from the Olduvai Basin, Tanzania (Olduvai Gorge Coring Project). Palaeogeography, Palaeoclimatology, Palaeoecology 571: 1-19.

31. Head MJ (2021) Review of the Early–Middle Pleistocene boundary and Marine Isotope Stage 19. Progress in Earth and Planetary Sci 8(50): 1-38.

32. Nur A, CF Helsey (1971) Paleomagnetism of Tertiary and Recent Lavas of Israel. Earth Planet Sci Lett 10(3): 375-379.

33. Ron H, R Freund, Z Garfunkel, A Nur (1984) Block rotation by strike-slip faulting: structural and paleomagnetic evidence. Jour of Geophysical Research 89P: 6256-6270.

34. Heimann A (1990) The development of the Dead Sea Rift and its margins in northern Israel during the Pliocene and Pleistocene. PhD Thesis, Hebrew University, Jerusalem (in Hebrew, summary in English) pp. 1-114.

35. Braun D, H Ron, M Marco (1991) Magnetostratigraphy of the hominid tool-bearing Erk el Ahmar Formation in the northern Dead Sea Rift. Israel Jour. of Earth Sci 40(1): 191-197.

36. Heimann A, D Braun (2000) Quaternary stratigraphy of the Kinnarot Basin, Dead Sea Transform, northeastern Israel. Israel Jour of Earth Sci 49(1): 31-44.

37. Ron H, N Porat, A Ronen, E Tchernov, LK Horwitz (2003) Magnetostratigraphy of the Evron Member – implications for the age of the Middle Acheulian site of Evron Quarry. Journal of Human Evolution 44(5): 633-639.

38. Dembo N, Y Hamiel, R Granot (2015) Intraplate rotational deformation induced by faults: Carmel-Gilboa fault system as a case study. Geological Survey of Israel, Report No. GSI/19/2015, Jerusalem pp. 32-40.

39. Probokormi MS, B Urban, S Mischke, HK Mienis, J Melamed, et al. (2018) Evidence for climatic changes around the Matuyama-Brunhes Boundary (MBB) inferred from a multi-proxy paleoenvironmental study of the GBY #2 core, Jordan River Valley, Israel. Palaeogeography, Palaeoclimatology, Palaeoecology 489(1): 166-185.

40. Behar N, R Shaar, L Tauxe, H Asefaw, Y Ebert, et al. (2019) Paleomagnetism and paleosecular variations from the Plio-Pleistocene Golan Heights volcanic plateau, Israel. Geochemistry, Geophysics, Geosystems 20(1): 4319-4335.

41. Scardia G, F Parenti, DP Miggins, Axel Gerdes, Astolfo GM Araujo, et al. (2019) Chronologic constraints on hominin dispersal outside Africa since 2.48 Ma from the Zarqa Valley, Jordan. Quaternary Science Reviews 219(1): 1–19.

42. Larrasoaña JC, N Waldmann, S Mischke, J Avni, H Ginat (2020) Magnetostratigraphy and Paleoenvironments of the Kuntila Lake Sediments, Southern Israel: Implications for Late Cenozoic Climate Variability at the Northern Fringe of the Saharo-Arabian Desert Belt. Frontiers in Earth Sciences 173(1): 1-12.

43. Mor D, Steinitz G (1982) K-Ar age of the cover basalts surrounding the Sea of Galilee. Geol. Survey of Israel, Rep Me/6/82: 1-14.

44. Opdyke ND, N Lindsay, G Kukla (1983) Evidence for earlier date of Ubeidiya, Israel hominid site. Nature 304(28): 375-380.

45. Heimann A, G Steinitz (1989) Fault systems in the south-western Hula Valley and the eastern slopes of the Galilee – dating and tectonic implications. Trans. of the Israel Geol. Soc. Meet., Ramot, Israel, 2-5 April 1989(1): 73-75.

46. Mor DA (1993) A time-table for the Levant Volcanic Province, according to K-Ar dating in the Golan Heights, Israel. Jour of African Earth Sci 16(3): 223-234.

47. Heimann A, G Stenitz, D Mor, G Shaliv (1996) The Cover Basalt Formation, its age and its regional and tectonic setting: Implications from K-Ar and 40Ar/39Ar geochronology. Israel Jour of Earth Sci 45(1): 55-71.

48. Mor D, H Mihelson, Y Druckman, Y Mimran, A Heimann, M Goldberg, A Sneh (1997) Notes on the geology of Golan Heights. Report of Geol. Survey of Israel 15/97, Jerusalem pp. 1-18.

49. Segev A (2000) Synchronous magmatic cycles during the fragmentation of Gondwana: Radiometric ages from the Levant and other provinces. Tectonophysics 325(3-4): 257-277.

50. Segev A, Lang B (2002) 40Ar/39Ar dating of Valanginian top Tayasir Volcanics in the Mount Hermon area, northern Israel. Israel Geological Survey, Current Research 13(1): 100-104.

51. Ginat H, E Zilberman, I Saragusti (2003) Early Pleistocene lake deposits and Lower Paleolithic finds in Nahal (wadi) Zihor, Southern Negev desert, Israel. Quaternary Research 59(3): 445-458.

52. Weinstein Y, O Navon, R Altherr, M Stein (2006) The Role of Lithospheric Mantle Heterogeneity in the Generation of PlioPleistocene Alkali Basaltic Suites from NW Harrat Ash Shaam (Israel). Journal of Petrology 47(5): 1017-1050.

53. Freund R, Z Garfunkel, I Zak, M Goldberg, T Weissbrod, et al. (1970) A discussion on the structure and evolution of the Red Sea and the nature

of the Red Sea, Gulf of Aden and Ethiopia rift junction - The shear along the Dead Sea rift. Philosophical Transactions of the Royal Society 267(1): 69-85.

54. Marcus E, J Slager, S Ben-Zaken, IY Indik (1984) Zemah-1. Geological Completion Report 84/11. Oil Exploration Ltd, Israel pp. 128-130.

55. Marcus E, J Slager (1985) The sedimentary-magmatic sequence of the Zemah-1 well (Jordan-Dead Sea rift, Israel) and its emplacement in time and space. Israel Jour of Earth Sciences 34(1): 1-10.

56. Rotstein Y, Y Bartov (1989) Seismic reflection across a continental transform: an example from a convergent segment of the Dead Sea rift. Jour of Geophysical Research 94(1): 2902-2912.

57. Shaliv G (1991) Stages in the tectonics and volcanic history of the Neogene basalt in the Lower Galilee and the valleys. PhD Thesis. Hebrew University, Jerusalem, Israel (in Hebrew, summary in English) pp. 112-150.

58. Ben-Avraham Z, U ten Brink, R Bell, M Reznikov (1996) Gravity field over the Sea of Galilee: evidence for a composite basin along a transform fault. Jour of Geophysical Research 101(B1): 533-544.

59. Hurwitz S, Z Garfunkel, Y Ben Gai, M Reznikov, Y Rotstein, et al. (2002). The tectonic framework of a complex pull-apart basin: seismic reflection observations in the Sea of Galilee, Dead Sea transform. Tectonophysics 359(3-4): 289-306.

60. Hall JK, VA Krasheninnikov, F Hirsch, C Benjamini, A Flexer (2005) Geological Framework of the Levant. Vol. II: The Levantine Basin and Israel. Historical Productions-Hall, Jerusalem, Israel pp. 826-850.

61. Schattner U, R Weinberger (2008) A mid-Pleistocene deformation transition in the Hula basin, northern Israel: Implications for the tectonic evolution of the Dead Sea Fault. Geochemistry, Geophysics, Geosystems 9(7): 1-18.

62. Eppelbaum LV, YuI Katz (2015) Eastern Mediterranean: Combined geological-geophysical zonation and paleogeodynamics of the Mesozoic and Cenozoic structural-sedimentation stages. Marine and Petroleum Geology 65(1): 198-216.

63. Segev A (2017) Zemah-1, a unique deep oil well on the Dead Sea fault zone, northern Israel: A new stratigraphic amendment. Geological Survey of Israel, Report GSI/21/2017 Jerusalem pp. 1-27.

64. Eppelbaum LV, Z Ben Avraham, Y Katz, S Cloetingh, M Kaban (2021) Giant quasi-ring mantle structure in the African-Arabian junction: Results derived from the geological-geophysical data integration. Geotectonics 55(1): 67-93.

65. Feibel CS (2004) Quaternary lake margins of the Levant Rift Valley. In Goren Inbar N, Speth JD (eds.), Human Paleoecology in the Levantine Corridor. Oxbow Books, Oxford pp. 21-36.

66. Tchernov E, Horwitz LK, Ronen A, A Lister (1994) The Faunal Remains from Evron Quarry in Relation to Other Lower Paleolithic Hominid Sites in the Southern Levant. Quaternary Research 42(3): 328-339.

67. Almogi-Labin A, Siman Tov R, Rosenfeld A, E Debard (1995) Occurrences and distribution of the foraminifer Ammonia beccari tepida (Cushman) in water bodies, recent and quaternary of the Dead Sea rift, Israel. Marine Micropaleontology 26(1): 153-159.

68. Bandel K, N Sivan, J Heller (2007) Melanopsis from Al-Qarn, Jordan Valley (Gastropoda: Gerithioidea). Palaontologische Zeitschrift 81(3): 304-315.

69. Leakey MG, L Werdelin (2010) Early Pleistocene Mammals of Africa: Background to Dispersal. In: (Fleagle, J.G. et al., Eds.). The First Hominin Colonization of Eurasia, Springer, Dordrecht – Heidelberg – London, UK pp. 3-11.

70. Rabinovich R, G Herzlinger, R Calvo, F Rivals, S Mischke, et al. (2019) Erq el Ahmar Elephant Site – A mammoth skeleton at a rare and controversial Plio-Pleistocene site along the mammal migration route out of Africa. Quaternary Science Reviews 221(105885): 1-17.

71. Sneh A, Y Bartov, T Weissbrod, M Rosensaft (1998) Geological Map of Israel, 1:200,000 (4 sheets), Geological Survey of Israel, Jerusalem, Israel.

72. Bogoch R, A. Sneh (2008) Sheet 4-I, Arbel. Geological Map of Israel, Scale 1:50,000. Geological Survey of Israel, Jerusalem, Israel.

73. Sneh A. (2017) Sheet 4-II, Teverya. Geological Map of Israel, Scale 1:50,000. Geological Survey of Israel, Jerusalem, Israel.

74. Sneh A (2018) Sheet 3-IV, Nazerat. Geological Map of Israel, Scale 1:50,000. Geological Survey of Israel, Jerusalem, Israel.

75. Stekelis M, D Gilead (1967) Ma'ayan Barukh: A Lower Palaeolithic site in Upper Galilee. Mitekufat Haeven 8(1): 1-22.

76. Bar Yosef O, N Goren Inbar (1993) The Lithic Assemblages of 'Ubeidiya: A Lower Paleolithic Site in the Jordan Valley. Oedem 45(1): 1-266.

77. Goren-Inbar N, CS Feibel, KL Verosub, Y Melamed, ME Kislev, et al. (2000) Pleistocene Milestones on the Out-of-Africa Corridor at Gesher Benot Ya'aqov, Israel. Science 289(5481): 944-947.

78. Mallol C (2006) What's in a beach? Soil micromorphology of sediments from the Lower Paleolithic site of 'Ubeidiya, Israel. Journal of Human Evolution 51(2): 185-206.

79. El Zaatari S (2018) The central Levantine corridor: The Paleolithic of Lebanon. Quaternary International 466(Part A): 33-47.

80. Goren-Inbar N, N Alperson Afil, G Sharon, G Herzlinger (2018) The Acheulian site of Gesher Benot Ya'akov. Vol. IV. Springer, Cham, Switzerland pp. 456-500.

81. Trifonov VG, AS Tesakov, AN Simakova, DM Bachmanov (2019) Environmental and geodynamic settings of the earliest hominin migration to the Arabian-Caucasus region: A review. Quaternary International 534(1): 116-137.

82. Herzlinger G, M Brenet, A Varanda, M Deschamps, N Goren Inbar (2021) Revisiting the Acheulian Large Cutting Tools of 'Ubeidiya, Israel. Journal of Paleolithic Archaeology 4(31): 1-29.

83. Eppelbaum LV (2014) Geophysical observations at archaeological sites: Estimating informational content. Archaeological Prospection 21(2): 25-38.

84. Eppelbaum LV (2014) Four Color Theorem and Applied Geophysics. Applied Mathematics 5(1): 358-366.

85. Borda M (2011) Fundamentals in Information Theory and Coding. Springer, Berlin-Heidelberg pp. 504-510.

86. Hsü KJ, MB Citta, WBF Ryan (1972) The origin of the Mediterranean evaporites. In: (A.G. Kaneps, Editor), Initial Reports of the Deep-Sea Drilling Project, XIII (Part 2). U.S. Government Printing Office, Washington DC pp. 1203-1231.

87. Krijgsman W, W Capella, D, FJ Hilgen, TJ Kouwenhoven, PT Meijer, et al. (2018) The Gibraltar Corridor: Watergate of the Messinian Salinity Crisis. Marine Geology 403(1): 238-246.

88. Eppelbaum L, Z Ben-Avraham, Y Katz (2004) Integrated analysis of magnetic, paleomagnetic and K-Ar data in a tectonic complex region: an example from the Sea of Galilee. Geophysical Research Letters 31(19): 1-4.

89. Davis M, A Matmon, D Fink, H Ron, S Niedermann (2011) Dating Pliocene lacustrine sediments in the central Jordan Valley, Israel – Implications for cosmogenic burial dating. Earth and Planetary Science Letters 305(3-4): 317-327.

90. Ronen A (1991) The Lower Palaeolithic Site Evron-Quarry in Western Galilee, Israel. Sonderveröffentlichungen Geologisches Institut der Universität zu Köln 82(2): 187-212.

91. Molostovsky EA, DM Pechersky, IYu Frolov (2007) Magnetostratigraphic Timescale of the Phanerozoic and Its Description Using a Cumulative Distribution Function. Izvestiya, Physics of the Solid Earth 43(10): 811–818.

92. Pechersky DM, AA Lyubushin, ZV Sharonova (2010) On the synchronism in the events within the core and on the surface of the earth: the changes in the organic world and in the polarity of the geomagnetic field in the Phanerozoic. Izvestiya, Physics of the Solid Earth 46(3): 613-623.

93. Bosworth W, P Huchon, K McClay (2005) The Red Sea and Gulf of Aden basins. Jour of African Earth Sciences 43(1-3): 334-378.

94. Eppelbaum LV, Katz YI (2023) Combined paleomagnetic, paleogeographic, and event stratigraphy studies increase the age of the anthropological site 'Ubeidiya in the Levantine Corridor (northern Israel) by 1.0 Ma. Trans of the 18th EUG Meet, Geophysical Research Abstracts, Vienna, Austria 25(1): EGU23-1598.

DOI: 10.32474/JAAS.2023.08.000286